PERGAMON

Deep-Sea Research II 49 (2002) 2345–2376

DEEP-SEA RESEARCH
PART II

www.elsevier.com/locate/dsr2

Microbial community dynamics and taxon-specific phytoplankton production in the Arabian Sea during the 1995 monsoon seasons

S.L. Brown[a,*], M.R. Landry[a], S. Christensen[a], D. Garrison[b,1], M.M. Gowing[c], R.R. Bidigare[a], L. Campbell[d]

[a] *Department of Oceanography, School of Ocean Earth Science and Technology, University of Hawaii, Manoa, Honolulu, HI 96822, USA*

[b] *The National Science Foundation, Division of Ocean Sciences, Biological Oceanography Program, Room 725, 4201 Wilson Blvd., Arlington, VA 22230, USA*

[c] *Institute of Marine Sciences, University of California, Santa Cruz, CA 95064, USA*

[d] *Department of Oceanography, Texas A&M University, College Station, TX 77843, USA*

Received 7 June 2001; received in revised form 9 November 2001; accepted 1 December 2001

Abstract

As part of the US JGOFS Arabian Sea Process Study in 1995, we investigated temporal and spatial patterns in microbial dynamics and production during the late Southwest (SW) Monsoon (August–September 1995) and the early Northeast (NE) Monsoon (November–December 1995) seasons using the seawater-dilution technique. Experiments were coupled with population assessments from high-performance liquid chromatography, flow cytometry, and microscopy to estimate further taxon-specific phytoplankton growth, grazing and production. Dilution estimates of total primary production varied substantially, from 7 to 423 $\mu g\ C\ l^{-1}\ d^{-1}$, and were generally in good agreement with rate estimates from ^{14}C-uptake incubations. Both primary production and secondary bacterial production were, on average, 2.5 × higher during the SW Monsoon than the NE Monsoon. Relative to the total community, photosynthetic prokaryotes contributed 23% and 53% of production during the SW and NE Monsoons, respectively. *Prochlorococcus* spp. production was well balanced by grazing losses, while >50% of *Synechococcus* spp. production during the SW Monsoon appeared to escape grazing by protists. Diatoms comprised >30% of primary production at a high biomass station during the SW Monsoon but <30% at all stations during the NE Monsoon. Growth rates of *Synechococcus* spp. and diatoms appeared to be limited by inorganic nitrogen concentrations, while *Prochlorococcus* spp., dinoflagellates and *Phaeocystis* spp. were not. Losses to protistan grazing were strongly correlated with phytoplankton biomass and production. Despite sufficient prey levels, protistan biomass was modest and constant across the region during both seasons. Of the larger taxa, diatoms were grazed the least effectively with only 50% of daily production accounted for by protistan grazing. Combined estimates of protistan and mesozooplankton grazing at upwelling stations during the SW Monsoon leave ~10% of primary production unaccounted for and available for sinking and/or lateral advection. Similarly high rates of net production at northern coastal stations during the NE Monsoon suggest that this area also may contribute to regional export flux. © 2002 Published by Elsevier Science Ltd.

*Corresponding author.
E-mail address: sbrown@soest.hawaii.edu (S.L. Brown).

[1] Interpretations and conclusions are those of the author and do not imply the endorsement of the National Science Foundation.

0967-0645/02/$ - see front matter © 2002 Published by Elsevier Science Ltd.
PII: S0967-0645(02)00040-1

1. Introduction

The Arabian Sea is characterized by seasonally reversing monsoonal winds, resulting in alternating periods of quiescence and mixing due to upwelling during the Southwest (SW) Monsoon and convection during the Northeast (NE) Monsoon. These oscillations in physical forcing and periodic nutrient enhancement result in dramatic seasonal and spatial variations in biological communities and processes. As a consequence, the Arabian Sea is a natural laboratory for studying variability in microbial community structure and its link to production and physical forcing mechanisms.

The US Joint Global Ocean Flux Study (US JGOFS) Arabian Sea Process Study (ASPS) spanned the annual cycle of reversing winds during seven cruises in 1995, from the late NE Monsoon in January through the onset of the NE Monsoon in December. The ASPS provided numerous opportunities to document changes in microbial community structure and standing stocks. During Intermonsoon periods and offshore, generally warm nutrient-poor waters, unaffected by wind-driven upwelling or convection, were dominated by photosynthetic picoplankton, primarily *Prochlorococcus* spp. (Burkill et al., 1993a, b; Jochem et al., 1993; Campbell et al., 1998; Tarran et al., 1999; Garrison et al., 2000). During the SW Monsoon season, the dominance shifted to larger autotrophic nanoplankton and microplankton, particularly in the colder nutrient-rich waters inshore, where *Prochlorococcus* spp. were virtually absent (Burkill et al., 1993a, b; Garrison et al., 1998, 2000; Tarran et al., 1999; Shalapyonok et al., 2001). Spatial heterogeneity in phytoplankton distributions during the SW Monsoon season was linked to coastal filaments and mesoscale eddies, which transported coastal populations and upwelling influences to offshore sites (Brink et al., 1996; Garrison et al., 1998; Latasa and Bidigare, 1998; Manghnani et al., 1998; Flagg and Kim, 1998). Populations followed a similar onshore to offshore gradient of decreasing cell size during the NE Monsoon, which was characterized by low nutrient concentrations, increased temperatures, and deeper mixed layers (Morrison et al., 1998; Garrison et al., 2000). Heterotrophic bacterial biomass was relatively uniform in time and space, lacking much of the variability of the phytoplankton populations (Ducklow et al., 2001).

Despite substantial changes in microbial community composition and biomass, community

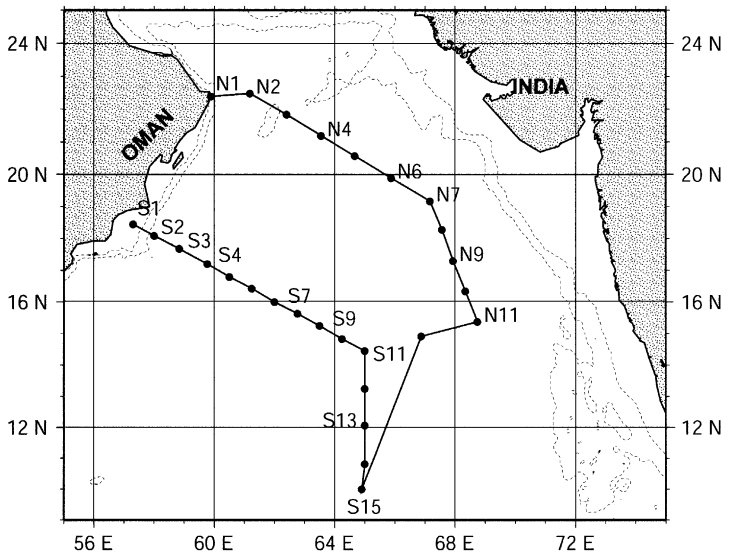

Fig. 1. Station map for US JGOFS Arabian Sea Process Study cruises TN050 (late Southwest Monsoon) and TN054 (early Northeast Monsoon) showing locations of study sites.

production did not differ as much as might be expected (Barber et al., 2001; Dickson et al., 2001). Based mainly on experiments conducted along the southern transect line (Fig. 1), Barber et al. (2001) concluded that primary productivity during Intermonsoon periods was markedly higher than for previously studied oligotrophic regions in the Pacific Ocean, and similar to that measured during the SW and NE Monsoon seasons. Similarly, Ducklow et al. (2001) found little enhancement (<2-fold) in bacterial secondary production rates during the monsoon seasons. Based on the lack of strong seasonal trends in production, changes in microbial biomass and community structure do not appear to parallel production, which may account for the apparent uncoupling between production and export (Buesseler et al., 1998a, b).

Considered independently, neither standing stocks nor growth rate estimates adequately represent production, and production alone does not necessarily scale with export flux. Here we present the first compilation of microbial stocks and rates in an effort to assess the magnitude, seasonal differences and spatial variability in microbial production during the 1995 monsoon seasons. We further consider taxon-specific phytoplankton growth and mortality rates in relation to physical forcing and protistan grazing to examine factors regulating microbial production. Finally, we partition phytoplankton production into component taxa and consider the fate of net production with a focus on linking microbial production and export flux.

2. Materials and methods

Temporal and spatial patterns in microbial growth, grazing and biomass were investigated in the Arabian Sea on cruises during the late SW Monsoon (SWM) season (TN050: August–September 1995) and the early NE Monsoon (NEM) season (TN054: November–December 1995). Both cruises followed the same track, starting and ending in Muscat, Oman, and including an onshore to offshore northern transect (N stations) and an offshore to onshore southern transect (S stations) (Fig. 1). Dilution experiments were conducted and analyzed by high-performance liquid chromatography (HPLC) and flow cytometry (FCM) to estimate group-specific growth and mortality due to protistan grazing. Rates were augmented by phytoplankton and micrograzer biomass estimates derived from microscopy. Details of the methodology are described below.

2.1. Dilution experiments

Dilution experiments were prepared according to Landry et al. (1998). All steps of experimental setup were done under trace-metal-clean techniques to avoid contamination. Polycarbonate bottles (2.1 l) were filled to establish a nutrient-rich, replicated, dilution series of 0.22, 0.45, 0.65, 0.86, and 1.0 natural (unfiltered seawater). Filtered water was first added to the bottles in measured amounts, and the remaining volume was gently filled with natural seawater from the same depth. To promote constant phytoplankton growth, each bottle received added nutrients for a final concentration of 0.5 μM ammonium, 0.03 μM phosphate, 1.0 nM $FeSO_4$ and 0.1 nM $MnSO_4$. Four experimental bottles also were filled with whole seawater without added nutrients. Two of these were used for initial samples; the other two were incubated as natural seawater controls. All bottles were incubated for 24 h in seawater-cooled shipboard incubators screened with neutral density fabric to achieve appropriate light levels.

2.2. High-performance liquid chromatography (HPLC)

Seawater samples for HPLC were analyzed according to Bidigare and Trees (2000). Samples of 1.7–2.1 l were pressure-filtered in a closed system through 25-mm Whatman GF/F glass-fiber filters. Filters were wrapped in aluminum foil, immediately frozen in liquid nitrogen, and stored at −80°C until analysis. Following disruption of cells by sonication, pigments were extracted in 3 ml of 100% acetone in the dark at 0°C for 24 h. Canthaxanthin (50 μl in acetone) was added as an internal standard to all samples. Prior to analysis, the pigment extracts were vortexed and centrifuged to remove cellular debris.

Samples (200 μl) of a mixture of 1.0 ml pigment extract and 0.3 ml H_2O were injected into a Varian 9012 HPLC system equipped with Varian 9300 autosampler, a Timberline column heater (26°C), and Spherisorb 5-μm ODS2 analytical column (4.6 × 250 mm) with a corresponding guard cartridge. Pigments were detected with a Thermo-Separation Products UV2000 absorbance (436 and 450 nm) detector. Separation of pigments was accomplished using a modified version of the ternary solvent protocol of Wright et al. (1991), with eluent A = 80:20 mixture of methanol:0.5 M ammonium acetate, eluent B = 85:15 mixture of acetonitrile:water and eluent C = ethyl acetate. Eluents A and B also contained 0.01% 2,6-di-tert-butyl-*p*-cresol (BHT) to prevent the conversion of chlorophyll *a* to its allomers. The linear gradient was 0′ (90% A, 10% B), 1′ (100% B), 11′ (78% B, 22% C), 27.5′ (10% B, 90% C), 29′ (100% B), 30′ (100% B), and the flow rate was 1 ml min^{-1}. Peak identifications were made by comparing retention times of eluting peaks with those of pure standards and extracts prepared from algal cultures of known pigment composition (Bidigare, 1991; Latasa and Bidigare, 1998). Total chlorophyll *a* (TChl*a*) is defined as the sum of chlorophyllide *a*, monovinyl chlorophyll *a* and divinyl chlorophyll *a*.

Stations were grouped according to the results of a pigment cluster analysis (MINITAB statistical package) following the criteria of Latasa and Bidigare (1998). Pigment clusters were re-analyzed for only the mixed layer, rather than the full depth profiles used previously. We used the same subset of 10 pigments (chlorophyllide *a*, peridinin, 19′-butanoyloxyfucoxanthin, 19′-hexanoyloxyfucoxanthin, fucoxanthin, zeaxanthin, lutein, prasinoxanthin, alloxanthin, and divinyl chlorophyll *a*), Manhattan distances between cases, and Ward's method for linkages between clusters. Stations during the SW (TN050) Monsoon were separated into four clusters: N1, N2, N4 and S7 (cluster 1); S2, S3 and S9 (cluster 2); S4 and S11 (cluster 3); and N6, N7, N11 and S15 (cluster 4). No pigment data were available for N1; but it was assigned to cluster 1 based on proximity and other shared characteristics with stations in this group. Stations from the NE Monsoon (TN054) fell into three main clusters: N9, N11, S15 and S13 (cluster 5); N1 and N2 (cluster 6); and N4, N6, N7, S11, S9, S7, S4, S3 and S2 (cluster 7).

2.3. Flow cytometry (FCM)

Subsamples (3 ml) were preserved in cryogenic tubes with paraformaldehyde (0.5% final concentration) and frozen in liquid nitrogen until analysis. In the laboratory, these samples were thawed and stained with Hoescht 33342 (0.8 μg ml^{-1} final concentration) for 30 min before analysis (Monger and Landry, 1993). Subsamples of 50 or 100 μl were enumerated on a Coulter EPICS 753 flow cytometer equipped with dual argon lasers and MSDS II automatic sampling. The lasers were aligned colinearly with the first laser tuned to the UV range to excite Hoechst-stained DNA. Blue fluorescence from the DNA stain was used to distinguish cells from nonliving particulate matter. The second laser was tuned to 488 nm at 1.0 W to excite the pigments of autotrophic cells. Microbial populations were distinguished by differences in forward-angle light-scatter (FALS) and fluorescence emission. Heterotrophic bacteria showed DNA-staining but no red fluorescence (680 ± 40 nm) due to chlorophyll. *Prochlorococcus* (PRO) showed small size (FALS) and red fluorescence. *Synechococcus* spp. (SYN) were identified based on orange fluorescence and small size. Larger photosynthetic eukaryotes (PEUKS) displayed greater light-scatter and red fluorescence. All FCM samples were spiked with a mixture of Polysciences Fluoresbrite YG 0.57- and 0.98 μm visible beads and 0.46 μm UV beads. Fluorescence per cell was normalized to the fluorescence values of the standard 0.57 μm beads for each identifiable phytoplankton population. Cell abundances were converted to biomass estimates using carbon-per-cell conversion factors determined for Arabian Sea populations (Shalapyonok et al., 2001; Garrison et al., 2000); carbon contents of 11, 32 and 101 fg C $cell^{-1}$ were used for heterotrophic bacteria, *Prochlorococcus* spp., and *Synechococcus* spp., respectively.

2.4. Microscopy

Water-column samples for microscopy were collected at various depths in the upper 100 m

from rosette sample bottles during standard hydrographic casts. Autotrophic and heterotrophic nanoplankton were enumerated according to Garrison et al. (1998). Replicate samples of 50–150 ml were concentrated on 0.8-μm black Poretics filters and stained with either DAPI or proflavin + DAPI. Glutaraldehyde (final concentration = 0.5%) and the stains were added when ~10 ml remained in the filter towers and allowed to sit for 10–15 min before completing filtration. Filters were frozen at −80°C until subsequent laboratory analysis. Slides were viewed with an Olympus BX-60 microscope using blue excitation for proflavin-stained cytoplasm and autofluorescence and UV excitation for DAPI-stained nuclei. Samples were counted at 500×, 750× or 1250× as appropriate to enumerate all cells >2 μm in diameter.

Additional aliquots were preserved with Lugol's iodine solution (125 ml) or buffered paraformaldehyde (250 ml) for analysis of microplankton including diatoms, silicoflagellates, dinoflagellates and ciliates. Samples were settled and examined with an Olympus IMT-2 inverted microscope. Concentrated DAPI (final concentration = 0.5 μg ml^{-1}) was added to settled paraformaldehyde samples for analysis with UV excitation, and autofluorescence was determined with blue excitation. Lugol's samples were viewed with transmitted light.

Carbon estimates were derived from measured cell dimensions, appropriate geometric formulae, and carbon-to-volume ratios. Diatom and flagellate biovolumes (BV, μm^3) were converted to biomass (pg C) based on Eppley et al. (1970): $\log_{10}(\text{pg C}) = 0.76 \log_{10}(\text{BV}) - 0.35$ and $\log_{10}(\text{pg C}) = 0.94\,1\log_{10}(\text{BV}) - 0.60$, respectively. Ciliate biovolume (BV, μm^3) was converted to biomass using pg C = 0.16 BV and pg C = 0.19 BV for samples preserved with paraformaldehyde and Lugol's, respectively (Putt and Stoecker, 1989). For *Phaeocystis* colonies, the number of cells per colony was estimated as a function of colony volume using $\log_{10}(\text{Colony cell number}) = 0.51 (\log_{10}[\text{Colony volume, mm}^3] + 3.61)$ (Rousseau et al., 1990), and biomass was determined from abundance using 8.6 pg C cell^{-1} derived from the Eppley et al. (1970) equation for nondiatoms. The difference between the total number of photosynthetic eukaryotes (PEUKS) from FCM and the total number of cells >2 μm enumerated from microscopy was used to account for cells that were missed by microscopy (PICOS), whether due to small size or preservation and filtration artifacts. As these cells are largely comprised of true picoeukaryotes (<2 μm) and slightly larger cells, we assumed an average cell diameter of 2.5 μm and 1810 pg C cell^{-1}. During the SW Monsoon (TN050), however, distinct populations of smaller eukaryotes were distinguishable by FCM at stations N2 and S2.

2.5. Rate estimates

HPLC pigment concentrations and FCM phytoplankton abundances were determined from measured concentrations inside the initial bottles, the filtered water carboy, and the volumes of natural and filtered water in the dilution mixtures. Net rates of change (k_i, d^{-1}) for total community and specific functional groups were determined for each experimental treatment. Linear regressions of net growth rate against dilution factor (D_i = proportion of natural seawater in the dilution treatment) for the nutrient-enriched treatments yielded estimates of phytoplankton growth (μ_n, growth with nutrients = Y-axis intercept) and phytoplankton mortality due to grazing (m = regression slope). It should be noted that D_i is assumed to represent the dilution effect on grazer abundance, a proxy for the relative grazing rate (R). For this reason, errors in the estimation of the dilution factor can affect significantly the calculation of mortality rates (Landry, 1993). Nonetheless, tests of this assumption in the equatorial Pacific Ocean have shown a significant 1:1 relationship between sample dilution and measures of relative grazing activity (Landry et al., 1995), making our estimates of dilution factors adequate, although not optimal. Phytoplankton growth without added nutrients (μ_0) was computed from the sum of grazing mortality (m) and mean growth rate (k_0) in the unamended seawater treatments (i.e., $\mu_0 = k_0 + m$). The ratio of μ_0 to μ_n (μ_0/μ_n) is an index of nutrient-limited growth.

Dilution experiments were usually conducted at two depths within the seasonal mixed layer, representing ~60% and 20% of photosynthetically active radiation (PAR). Seasonal mixed-layer depths (MLD) were determined from the depth of a 0.25 kg m^{-3} density increase from surface density (Gardner et al., 1999). Rate estimates and physical properties from depths corresponding to the two light intensities showed little variation and were averaged to represent the surface mixed layer.

Mortality rates were assumed to be unaffected by physiological changes in the phytoplankton during incubations (Landry et al., 2002), whereas pigment-based growth rates may have been influenced by adaptations to light level (Goericke and Welschmeyer, 1992a, b; Waterhouse and Welschmeyer, 1995). Likewise, growth-rate inferences based on changes in cell abundance do not account for changes in cell biovolumes. To correct for potential cell size adjustments of PRO and SYN, we used $0.56 \times$ FALS as a relative measure of the changes in cell biovolumes in unamended whole seawater incubations (Landry et al., submitted). This estimation is based on the assumption that FALS is directly proportional to (Biovolume)$^{\beta}$ (Binder et al., 1996) and that β is 1.83 (Morel, 1991). Such adjustments were generally <10% of growth rate estimates. To correct HPLC pigment-based estimates of *Prochlorococcus* spp. growth rates (DIVA), we used FCM measurements of cellular red fluorescence in initial and final samples to assess the rate of change of divinyl chlorophyll *a* due to photoadaptation. Similarly, FCM-derived changes in cellular fluorescence of PEUKS were used to correct growth rates for eukaryotes derived from HPLC monovinyl chlorophyll *a* and other diagnostic pigments.

Instantaneous rates of group-specific growth and grazing mortality, derived from HPLC and FCM, were used to compute group-specific biomass production (PP, μg C l^{-1} d^{-1}) and grazing losses (G, μg C l^{-1} d^{-1}) according to the following equations (Landry et al., 2000):

$$\mathrm{PP} = \mu_0 C_m$$

$$G = mC_m$$

and

$$C_m = C_0[e^{(\mu-m)t} - 1]/(\mu_0 - m)t,$$

where C_m is the average concentration of group-specific carbon during the experiment and C_0 is the initial group-specific biomass determined from FCM and/or microscopical analyses. When μ and m estimates for these calculations were based on pigment inferences rather than FCM, the C:pigment ratio was assumed to remain constant during the incubation.

3. Results

3.1. Hydrography

Smith et al. (1998a, b) and Morrison et al. (1998) described the physical and chemical environment during the 1995 monsoon seasons. Upwelling was apparent along the Omani coast during the late SW Monsoon (TN050), creating a gradient from low-temperature, high-nutrient water inshore to warmer, nutrient-depleted waters offshore (Table 1). In addition, strong, jet-like currents ran offshore from the area of coastal upwelling as mesoscale eddies dominated the region, extending the influence of the upwelling 500–700 km offshore and contributing to the hydrographic variability (Dickey et al., 1998; Flagg and Kim, 1998; Morrison et al., 1998; Lee et al., 2000). Surface temperatures ranged from 22.4°C at stations closest (5 km) to the coastline to 28.1°C offshore. Surface nitrate and silicate concentrations ranged from below the limit of detection to 20.6 μM and from 0.2 to 13.7 μM, respectively. Total chlorophyll *a* (TCHL *a*) concentrations ranged an order of magnitude from 138 ng l^{-1} offshore to 1600 ng l^{-1} at coastal station N1.

At the onset of the NE Monsoon (TN054), mixed-layer depths increased due to surface cooling and convection (Table 1). Compared to the late SW Monsoon (TN050), surface temperatures varied little over the study area, ranging only from 25.7°C to 28.2°C. Nutrient concentrations were lower and more uniform, with nitrate varying from 0.06 to 3.1 μM and silicate ranging from 1.6 to 4.0 μM. TCHL *a* concentrations during the NE

Table 1
Summary of environmental parameters for ASPS stations

Cruise	STA	Km	Z(m)	ML(m)	$T°C$	NO_3	PO_4	NH_4	Si	TCHL *a*
SWM	N1	5	10	38	22.4	18.2	1.70	0.64	8.7	1600[a]
SWM	N2	138	5,15	24	24.4	11.5	1.20	0.15	5.0	829
SWM	N4	424	7,20	52	27.0	0.3	0.48	0.19	0.8	709
SWM	N6	707	9,25	56	27.6	0.1	0.42	0.02	0.8	264
SWM	N7	862	10,25	48	28.0	0.0	0.37	0.00	1.3	138
SWM	N11	1319	25	58	28.1	0	0.30	0.02	1.0	202
SWM	S15	1492	10,30	105	27.8	0.2	0.31	0.01	0.3	214
SWM	S11	997	6,16	84	27.0	0	0.38	0.17	0.2	618
SWM	S9	813	25	95	26.5	3.3	0.59	0.17	2.4	459
SWM	S7	630	7,18	50	26.6	3.2	0.62	0.33	2.3	661
SWM	S4	359	6,15	24	25.0	8.1	0.92	0.34	2.1	604
SWM	S3	246	12	12	23.4	13.3	1.28	0.61	2.8	401
SWM	S2	147	5,15	16	23.2	14.9	1.36	0.63	4.3	406
SWM	S1	61	12	11	20.3	20.6	1.78	0.20	13.7	1444
NEM	N1	5	10	58	25.7	2.7	0.60	0.72	3.0	621
NEM	N2	138	8,16	34	25.7	3.1	0.58	0.28	2.3	611
NEM	N4	424	7,48	64	26.7	1.7	0.54	0.18	1.8	373
NEM	N6	701	9	64	27.2	0.3	0.35	0.01	2.8	377
NEM	N7	862	8,19	64	27.2	0.1	0.35	0.00	3.8	542
NEM	N9	1088	5	50	27.5	0.1	0.32	0.00	3.1	201
NEM	N11	1319	6	70	27.7	0.1	0.36	0.02	3.1	189
NEM	S15	1492	9,50	72	28.2	0.1	0.31	0.00	1.6	309
NEM	S13	1262	6	72	28.0	0.1	0.33	0.00	2.4	307
NEM	S11	997	7,23	82	27.7	0.1	0.29	0.00	2.9	416
NEM	S9	813	5	76	27.2	0.3	0.35	0.16	2.3	363
NEM	S7	630	5,25	58	26.7	1.5	0.49	0.19	2.2	412
NEM	S4	359	3,13	62	26.6	0.7	0.35	0.12	4.0	391
NEM	S3	246	5	62	26.5	0.2	0.33	0.10	3.0	361
NEM	S2	147	16	72	26.3	0.1	0.30	0.03	2.6	547

SWM = Southwest Monsoon (TN050), NEM = Northeast Monsoon (TN054), km = distance from shore in kilometers, Z = depth of experiments in meters, ML = mixed layer depth in meters, $T°C$ = temperature. All nutrient concentrations are in μM and TChl *a* represents HPLC-derived total chlorophyll *a* in ng chl l^{-1}.

[a] Concentration determined from different HPLC cast.

Monsoon reached a maximum of only 620 ng l^{-1} (station N1).

3.2. Community biomass and production

Phytoplankton community estimates of mixed-layer biomass, production and grazing rates are shown in Table 2. Carbon to chlorophyll *a* ratios (weight:weight) ranged from 44 to 153, and were slightly higher during the SW Monsoon (mean = 80) than the NE Monsoon (mean = 72). No clear spatial patterns were evident. For stations where biomass estimates from microscopy were not available, the average C:Chl *a* ratio for the appropriate station cluster (see Section 2.2) was used to estimate phytoplankton carbon from TCHL *a* concentrations. Phytoplankton biomass estimates ranged from 9 to 101 μg C l^{-1}, averaging 43 μg C l^{-1} during the SW Monsoon and 30 μg C l^{-1} in the NE Monsoon. During both seasons, phytoplankton biomass was highest inshore along both transects and lower at stations furthest offshore (Table 2).

Community production rates varied dramatically from 7 to 423 μg C l^{-1} d^{-1}, with higher mean estimates during the SW Monsoon (102 μg

Table 2
Biomass and production estimates for the total phytoplankton community in the mixed layer

Cruise	STA	TCHL *a*	C_0	PP	*G*	*G*/*P*	$\%C_0$
SWM	N1	1600	101	423	217	0.51	215
SWM	**N2**	**829**	**43**	**75**	**37**	**0.50**	**87**
SWM	**N4**	**709**	**46**	**48**	**44**	**0.92**	**95**
SWM	N6	264	23	19	16	0.85	72
SWM	**N7**	**138**	**21**	**31**	**16**	**0.51**	**75**
SWM	**N11**	**202**	**13**	**16**	**5**	**0.33**	**41**
SWM	**S15**	**214**	**9**	**7**	**5**	**0.68**	**53**
SWM	**S11**	**618**	**35**	**37**	**27**	**0.74**	**78**
SWM	**S9**	**459**	**37**	**114**	**38**	**0.34**	**102**
SWM	**S7**	**661**	**47**	**107**	**70**	**0.65**	**150**
SWM	**S4**	**604**	**57**	**129**	**75**	**0.58**	**131**
SWM	**S3**	**401**	**42**	**50**	**36**	**0.72**	**87**
SWM	**S2**	**406**	**54**	**205**	**100**	**0.49**	**184**
SWM	**S1**	**1444**	**74**	**161**	**75**	**0.47**	**102**
NEM	N1	621	48	85	34	0.40	72
NEM	N2	611	47	78	52	0.67	111
NEM	N4	373	30	36	14	0.40	47
NEM	N6	377	31	57	19	0.34	63
NEM	**N7**	**542**	**24**	**77**	**44**	**0.57**	**186**
NEM	N9	201	10	2	4	1.56	39
NEM	N11	189	9	4	5	1.23	54
NEM	**S15**	**309**	**15**	**12**	**9**	**0.76**	**57**
NEM	S13	307	15	25	12	0.47	76
NEM	**S11**	**416**	**22**	**30**	**19**	**0.64**	**89**
NEM	S9	363	29	68	24	0.35	81
NEM	**S7**	**412**	**47**	**75**	**44**	**0.58**	**93**
NEM	**S4**	**391**	**43**	**62**	**40**	**0.64**	**92**
NEM	S3	361	29	21	15	0.74	52
NEM	**S2**	**547**	**45**	**34**	**32**	**0.94**	**71**

SWM = Southwest Monsoon (TN050), NEM = Northeast Monsoon (TN054), total chlorophyll *a* (TCHL *a*) from HPLC is in $ng\,l^{-1}$. C_0 is phytoplankton biomass in $\mu g\ C\,l^{-1}$. Total phytoplankton production (PP) is the sum of production estimates from divinyl chlorophyll *a* (DIVA) and monovinyl chlorophyll *a* (Chl *a*). PP and *G* denote daily phytoplankton community production and losses due to protistan grazing ($\mu g\ C\,l^{-1}\,d^{-1}$), respectively. *G*/*P* is the ratio of grazing to production. $\%C_0$ represents the percent of standing stock lost to grazing. Bold font denotes stations with C_0 and C:Chl measured by FCM and microscopy.

$C\,l^{-1}\,d^{-1}$) than the NE Monsoon ($44\,\mu g\,l^{-1}\,d^{-1}$). Particularly during the SW Monsoon and to a lesser extent in the NE Monsoon, production followed a distinct onshore to offshore gradient (Fig. 2). Losses to protistan grazing also varied substantially, accounting for 33–150% of daily production (Table 2). On average, grazing accounted for 59% of production during the SW Monsoon and 68% during the NE Monsoon. Grazing losses followed the same onshore to offshore gradient (Fig. 2) and were highly correlated with production rates over both seasons ($G = 9 + 0.4$ PP; $r = 0.99$; $n = 29$).

3.3. Prokaryote biomass and production

FCM-estimates of *Prochlorococcus* spp. (PRO) biomass in the mixed-layer ranged from zero across much of the study area during the SW Monsoon to $8.1\,\mu g\ C\,l^{-1}$ at offshore stations during the NE Monsoon (Table 3). Average PRO biomass during the SW Monsoon was $1.2\,\mu g\ C\,l^{-1}$ versus $3.0\,\mu g\ C\,l^{-1}$ during the NE Monsoon. Divinyl chlorophyll *a* (DIVA) is a diagnostic pigment of PRO and thus changes in the pigment concentration can be a proxy for PRO growth and subsequent production. For the

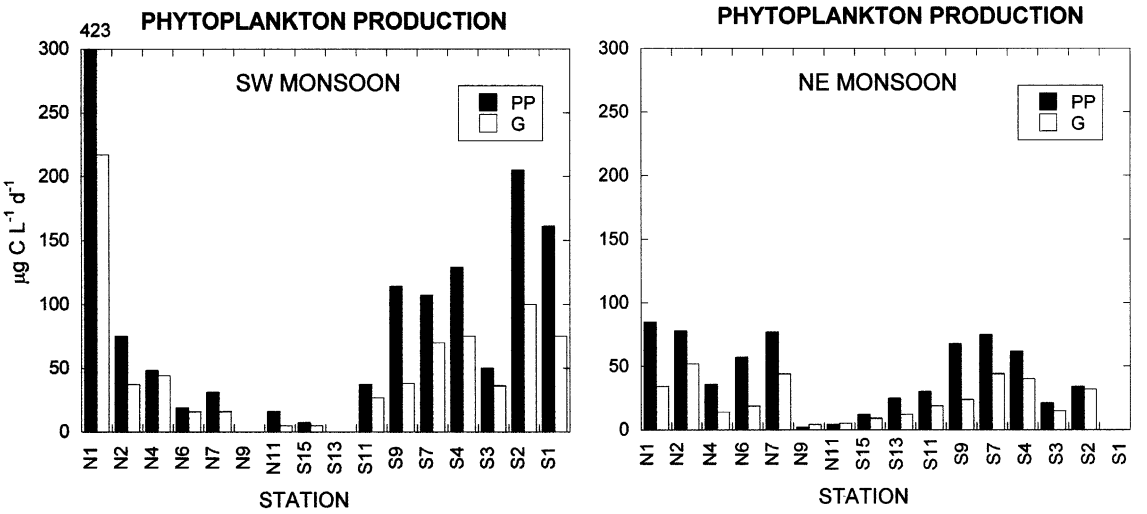

Fig. 2. Spatial distribution of total community daily primary production rates (PP) and grazing losses to protists (*G*) from dilution experiments in the surface mixed layer. Rates are based on the sum of HPLC-measured monovinyl and divinyl chlorophyll *a*.

stations where a comparison could be made between daily production estimates from PRO and DIVA, trends were similar although cell-based rates were slightly higher (mean difference = 0.6 μg $C l^{-1} d^{-1}$) (Table 4).

In general, PRO production estimates were modest, averaging 2.4 and 3.0 μg $C l^{-1} d^{-1}$ for the two seasons, depending on the parameter measured. Both parameters showed highest production (4.3–4.8 μg $C l^{-1} d^{-1}$) at station N7 (862 km offshore) during the SW Monsoon (Table 4). During the NE Monsoon, DIVA production was highest at stations >1000 km offshore, fairly constant inshore on the southern transect, and lowest close to the coast on the northern transect (Fig. 3). PRO estimates were also relatively constant inshore along the southern transect, with highest production rates offshore at station S13. PRO production constituted a minor fraction of total productivity (<10%) except at offshore stations where it reached ~20% during the SW Monsoon and ~45% during the NE Monsoon.

Grazing estimates from the two *Prochlorococcus* spp. parameters were 77% and 94% of daily production, averaged over both seasons. During the SW Monsoon, grazing losses accounted for 51% and 100% of production for PRO and DIVA, respectively, while during the NE Monsoon losses averaged 85–92%. Grazing equaled or exceeded growth at offshore stations during the NE Monsoon, particularly stations N9 and N11 (Fig. 3).

Synechococcus spp. (SYN) biomass varied over an order of magnitude, from 1.2 to 22.2 μg $C l^{-1}$ (Table 3). Biomass was higher at coastal stations and lower offshore during the NE Monsoon relative to the SW Monsoon. SYN exhibited a very different trend from PRO, with highest production rates on the northern transect and midway along the southern transect during both seasons (Fig. 3). Production rates were lowest at stations furthest offshore during both seasons and at southern stations adjacent to the coast. SYN production estimates were an order of magnitude higher than PRO, ranging broadly from <1 to 59 μg $C l^{-1} d^{-1}$ and averaging 13–14 μg $C l^{-1} d^{-1}$ (Table 4). SYN contribution to chl *a*-based estimates of total primary production varied markedly from <1% to 65% during the SW Monsoon and 7% to 158% during the NE Monsoon (Table 4). Grazing estimates accounted for <50% of production during the SW Monsoon with large imbalances at both northern and southern stations (Fig. 3). Grazing losses more

Table 3
Seasonal, spatial and taxonomic distributions of mixed-layer autotrophic carbon (μg $C l^{-1}$)

Cruise	STA	PRO	SYN	PICO	AF	PDINO	DIAT	Mphaeo	Cphaeo	Prok C	Euk C	AC	C:CHL
SWM	N1	0.0	**5.3**	—	—	—	—	—	—			100.8	63
SWM	N2	0.0	**7.8**	**28.6**	**1.8**	**0.7**	**3.1**	**0.0**	**1.1**	**7.8**	**35.2**	**43.0**	**52**
SWM	N4	0.0	**10.6**	**4.5**	**2.4**	**6.5**	**0.6**	**9.2**	**12.6**	**10.6**	**35.8**	**46.4**	**65**
SWM	N6	**0.0**	**13.0**	—	—	—	—	—	—	13.0	9.9	23.0	87
SWM	N7	**4.5**	**8.4**	**3.4**	**0.4**	**2.1**	**1.2**	**0.3**	**0.8**	**12.9**	**8.2**	**21.1**	**153**
SWM	N11	**3.5**	**3.1**	**1.7**	**0.4**	**1.7**	**0.2**	**0.6**	**1.8**	**6.6**	**6.3**	**12.9**	**64**
SWM	S15	**3.6**	**2.1**	**1.3**	**0.3**	**0.8**	**0.0**	**0.1**	**1.1**	**5.7**	**3.7**	**9.4**	**44**
SWM	S11	0.0	**2.9**	**2.1**	**1.5**	**2.0**	**10.5**	**0.2**	**14.0**	**2.9**	**32.1**	**35.0**	**57**
SWM	S9	0.0	**8.3**	**13.5**	**0.9**	**2.9**	**7.6**	**0.6**	**3.7**	**8.3**	**29.2**	**37.5**	**82**
SWM	S7	0.0	**14.3**	**12.4**	**2.9**	**2.3**	**4.9**	**0.5**	**9.3**	**14.3**	**32.3**	**46.6**	**71**
SWM	S4	0.0	**4.7**	**12.6**	**2.7**	**3.3**	**30.8**	**0.9**	**2.4**	**4.7**	**52.7**	**57.4**	**95**
SWM	S3	0.0	**3.2**	**15.4**	**2.3**	**9.0**	**8.7**	**0.2**	**2.7**	**3.2**	**38.4**	**41.6**	**104**
SWM	S2	0.0	**5.2**	**2.9**	**4.3**	**3.0**	**38.4**	**0.2**	**3.2**	**5.2**	**49.2**	**54.4**	**134**
SWM	S1	0.0	**2.1**	**16.8**	**7.5**	**18.1**	**25.2**	**0.0**	**3.9**	**2.1**	**71.5**	**73.7**	**51**
NEM	N1	0.0	**13.2**	—	—	—	—	—	—	**13.2**	34.6	47.8	77
NEM	N2	0.0	**22.2**	—	—	—	—	—	—	**22.2**	24.9	47.0	77
NEM	N4	**2.3**	**14.1**	—	—	—	—	—	—	**16.4**	13.8	30.2	81
NEM	N6	**3.1**	**4.1**	—	—	—	—	—	—	**7.2**	23.3	30.5	81
NEM	N7	**1.2**	**10.4**	**8.8**	**1.2**	**0.7**	**1.3**	—	—	**11.6**	**12.0**	**23.6**	**44**
NEM	N9	**5.6**	**7.5**	—	—	—	—	—	—	**13.1**	0.0	10.1	50
NEM	N11	**4.4**	**3.1**	—	—	—	—	—	—	**7.5**	1.9	9.5	50
NEM	S15	**8.1**	**1.2**	**3.7**	**1.2**	**1.1**	**0.1**	—	—	**9.3**	**6.1**	**15.4**	**50**
NEM	S13	**6.8**	**3.0**	—		—	—	—	—	**9.8**	5.5	15.4	50
NEM	S11	**2.1**	**7.3**	**9.6**	**1.2**	**1.2**	**0.6**	—	—	**9.4**	**12.6**	**21.9**	**53**
NEM	S9	**1.6**	**12.9**	—		—	—	—	—	**14.5**	14.9	29.4	81
NEM	S7	**1.9**	**17.9**	**23.2**	**1.4**	**1.9**	**1.0**	—	—	**19.8**	**27.5**	**47.3**	**115**
NEM	S4	**3.1**	**13.3**	**22.1**	**1.1**	**2.2**	**1.2**	—	—	**16.4**	**26.6**	**43.0**	**110**
NEM	S3	**2.8**	**10.9**	—	—	—	—	—	—	**13.7**	15.5	29.2	81
NEM	S2	**2.6**	**10.2**	**24.2**	**1.4**	**3.7**	**2.6**	—	—	**12.7**	**31.9**	**44.6**	**82**

SWM = Southwest Monsoon (TN050), NEM = Northeast Monsoon (TN054). PRO = *Prochlorococcus* spp., SYN = *Synechococcus* spp., PICO = picoeukaryotes, AF = autotrophic flagellates, PDINO = photosynthetic dinoflagellates, DIAT = diatoms, MPhaeo = motile *Phaeocystis* spp. CPhaeo = Colonial *Phaeocystis* spp., Prok C = prokaryote biomass, Euk C = eukaryote biomass, and AC = autotrophic carbon. C:CHL represents the weight ratio of AC to total chlorophyll *a*. Numbers in bold represent estimates from FCM and microscopy. Other estimates are described in text.

closely matched production during the NE Monsoon (average = 77%), particularly along the southern transect, while an imbalance remained in the north.

Photosynthetic prokaryotes as a whole (PRO + SYN) constituted a greater percentage of biomass during the NE Monsoon, accounting for nearly all of phytoplankton carbon at offshore, northern stations N9 and N11 and all across the southern transect (Table 3). During the SW Monsoon, photosynthetic prokaryotes dominated the biomass only at offshore stations N6-S15 and contributed $<20\%$ inshore. Total prokaryote production was only slightly higher during the NE Monsoon than the SW Monsoon (17 versus 14 μg $C l^{-1} d^{-1}$), comprising 25% and 59% of production during the SW and the NE Monsoons, respectively. Grazing losses averaged 60% of daily prokaryote production, accounting for 41% during the SW Monsoon and 78% during the NE Monsoon.

3.4. Eukaryote biomass and production

Eukaryotic autotrophs, comprised primarily of various flagellates, dinoflagellates, diatoms and the

Table 4
Production and grazing estimates from different prokaryotic parameters averaged over the mixed layer

Cruise	STA	PRO				DIVA				SYN			
		P	%TP	*G*	*G*/*P*	*P*	%TP	*G*	*G*/*P*	*P*	%TP	*G*	*G*/*P*
SWM	N1	—	—	—	—	—	—	—	—	20.6	5	0	0
SWM	N2	—	—	—	—	—	—	—	—	14.1	19	5.1	0.36
SWM	N4	—	—	—	—	—	—	—	—	13.9	29	3.6	0.26
SWM	N6	1.3	7	0.8	0.62	1.2	6	1.2	1.00	12.7	65	7.6	0.60
SWM	N7	4.8	16	2.1	0.44	4.3	14	4.0	0.92	3.2	10	1.8	0.59
SWM	N11	4.7	29	1.3	0.27	3.6	22	1.4	0.39	0	0	0.9	—
SWM	S15	2.3	32	1.6	0.72	0.9	12	1.6	1.76	3.4	0	1.4	0.42
SWM	S11	—	—	—	—	—	—	—	—	6.7	18	1.4	0.20
SWM	S9	—	—	—	—	—	—	—	—	21.0	18	4.1	0.20
SWM	S7	—	—	—	—	—	—	—	—	59.2	55	15.5	0.26
SWM	S4	—	—	—	—	—	—	—	—	9.3	7	3.7	0.40
SWM	S3	—	—	—	—	—	—	—	—	2.4	5	3.3	1.34
SWM	S2	—	—	—	—	—	—	—	—	15.1	7	6.3	0.42
SWM	S1	—	—	—	—	—	—	—	—	9.6	6	1.7	0.18
NEM	N1	—	—	—	—	—	—	—	—	33.8	40	11.5	0.34
NEM	N2	—	—	—	—	—	—	—	—	31.8	41	18.3	0.58
NEM	N4	2.7	8	1.6	0.61	1.1	3	0.9	0.81	31.1	87	22.0	0.71
NEM	N6	5.3	9	1.7	0.31	2.6	5	0.6	0.23	17.1	30	3.1	0.18
NEM	N7	1.3	2	0.9	0.69	1.3	2	1.2	0.97	13.2	17	7.5	0.57
NEM	N9	0.8	32	1.6	1.94	2.1	84	3.8	1.82	5.7	230	4.3	0.76
NEM	N11	1.4	34	2.0	1.48	1.8	43	2.9	1.66	2.9	69	2.3	0.78
NEM	S15	4.6	39	4.3	0.94	4.2	36	3.7	0.87	0.8	7	0.4	0.53
NEM	S13	7.4	30	4.6	0.63	5.7	23	5.3	0.93	7.0	28	2.5	0.36
NEM	S11	2.1	7	1.0	0.48	2.8	9	1.6	0.56	11.9	40	6.1	0.51
NEM	S9	2.4	4	2.0	0.83	0.5	1	0.5	0.89	28.5	42	22.2	0.78
NEM	S7	1.9	3	1.7	0.93	2.2	3	1.6	0.73	16.2	22	15.6	0.96
NEM	S4	3.3	5	1.8	0.55	2.8	5	1.9	0.66	6.0	10	6.0	1.00
NEM	S3	2.2	11	1.9	0.89	2.0	10	1.8	0.90	1.9	9	5.2	2.71
NEM	S2	2.3	7	1.8	0.80	1.9	6	1.7	0.89	7.3	21	5.8	0.80

SWM = Southwest Monsoon (TN050), NEM = Northeast Monsoon (TN054). PRO = *Prochlorococcus* spp., DIVA = divinyl chlorophyll *a*, SYN = *Synechococcus* spp. *P* = daily taxon-specific production and *G* = losses to microzooplankton grazing, both in $\mu g\ C\ l^{-1}\ d^{-1}$. %TP denotes the percent of total phytoplankton production attributed to each group. *G*/*P* is the ratio of grazing losses to daily production.

prymnesiophyte *Phaeocystis* spp., accounted for >80% of the phytoplankton biomass during the SW Monsoon, with the exception of the offshore stations N6-S15. During the NE Monsoon, eukaryotic biomass was relatively less important, generally representing <50% of phytoplankton biomass (Table 3).

Photosynthetic dinoflagellates (PDINO) were ubiquitous throughout the study region during both seasons; biomass maxima at stations S1, S3 and N4 during the SW Monsoon accounted for ~25% of phytoplankton carbon (Table 3). Microscopical estimates were not available for all stations; thus, the relationship between the diagnostic pigment peridinin (PER) and PDINO for the 18 stations with microscopy data was used to estimate PDINO biomass for the remaining stations (PDINO $\mu g\ C\ l^{-1} = 2.6 + 0.05[\text{PER ng}\ l^{-1}]$; $r = 0.88$; $n = 18$). Dinoflagellate production, estimated from synthesis and loss rates of PER, was greatest along the southern transect during the SW Monsoon ($23\ \mu g\ C\ l^{-1}\ d^{-1}$ at S3) (Fig. 4). Grazing losses of PDINO to microzooplankton averaged 76% of production during the SW Monsoon and 58% during the NE Monsoon, with substantial excess production at station S3 (SW Monsoon)

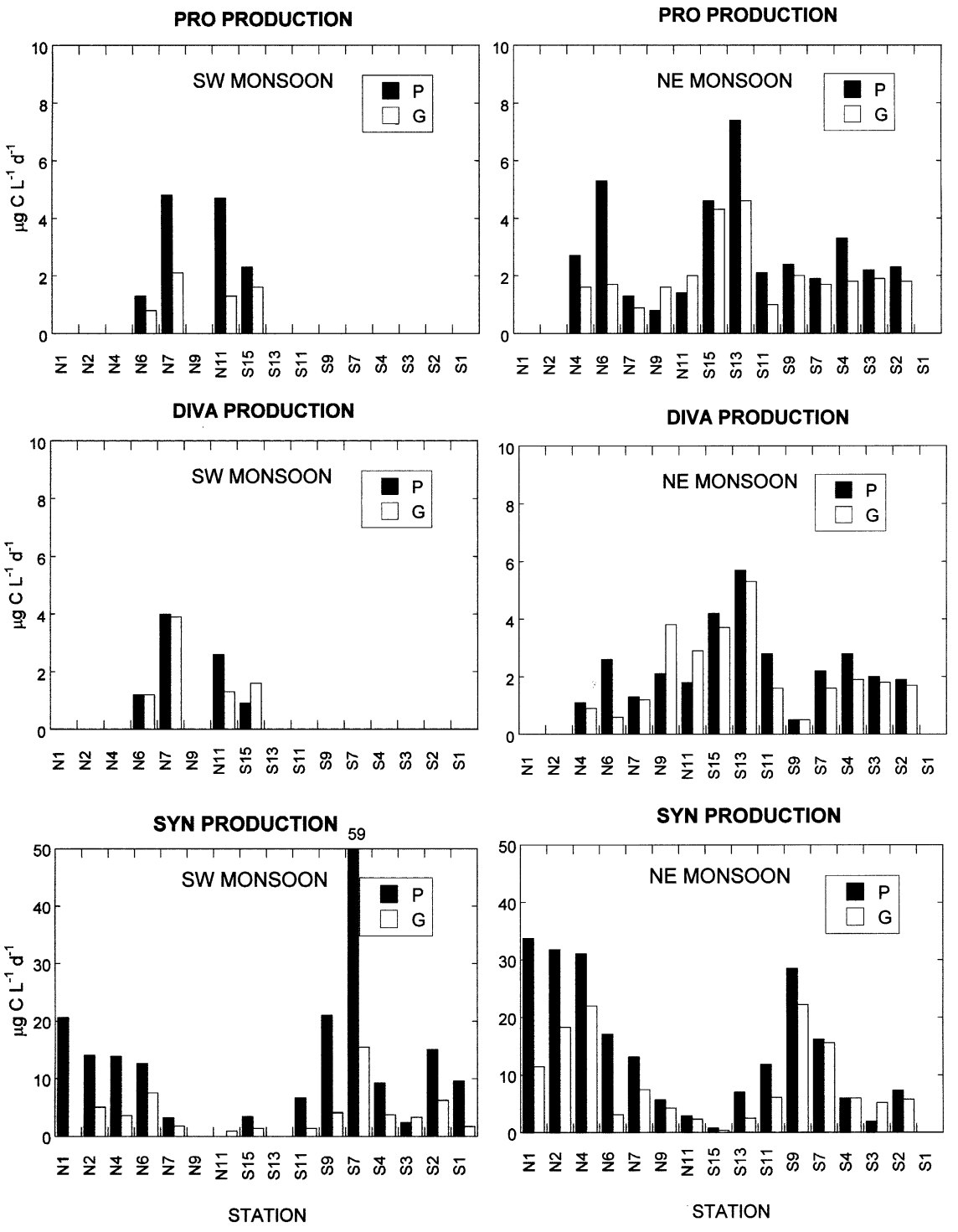
PRO PRODUCTION
SW MONSOON
P
G
µg C L-1 d-1
0
2
4
6
8
10
N1 N2 N4 N6 N7 N9 N11 S15 S13 S11 S9 S7 S4 S3 S2 S1
PRO PRODUCTION
NE MONSOON
P
G
DIVA PRODUCTION
SW MONSOON
P
G
DIVA PRODUCTION
NE MONSOON
P
G
SYN PRODUCTION
59
SW MONSOON
P
G
0
10
20
30
40
50
STATION
SYN PRODUCTION
NE MONSOON
P
G
STATION

and S9 (Table 5). With the exception of the high biomass at S3, PDINO generally contributed $<10\%$ of total daily production (Table 5).

Diatom biomass (DIAT) was high (up to 38.4 μg $C\,l^{-1}$), particularly along the southern transect, during the SW Monsoon and was low during the NE Monsoon (<3 μg $C\,l^{-1}$) except at the two northern coastal stations (Table 3). Fucoxanthin (FUCO) concentrations, a characteristic pigment of diatoms, were used to estimate DIAT biomass at stations lacking microscopical data according to the relationship DIAT (μg $C\,l^{-1}$) $= 0.3 + 0.8$ [FUCO ng l^{-1}] ($r = 0.66$; $n = 18$) for stations with measured biomass. Fucoxanthin is also present in some *Phaeocystis* spp. (Latasa and Bidigare, 1998); however, pigment ratios of three cultured Arabian Sea diatoms and one *Phaeocystis* spp. showed at least a 3-fold higher ratio of fucoxanthin to chl *a* in diatom species, indicating that diatoms accounted for most of the FUCO.

FUCO-based production estimates for diatoms ranged over two orders of magnitude from <1 to 234 μg $C\,l^{-1}\,d^{-1}$ and were highest along the southern line during the SW Monsoon (Table 5). During the NE Monsoon, production was <4 μg $C\,l^{-1}\,d^{-1}$ (Fig. 5), except for the northern coastal stations. These same areas of high diatom biomass showed diatom contributions were $>30\%$ of total phytoplankton production (PP), with estimates of $>50\%$ of PP only at stations S2-S4 during the SW Monsoon (Table 5). Grazing losses to protists averaged 45% of production during the SW Monsoon and 60% during the NE Monsoon.

Prymnesiophyte algae (PRYM), or more notably *Phaeocystis* spp. (PHAEO), were substantial contributors to phytoplankton biomass at stations N4, S7 and S11 during the SW Monsoon (Table 3). Because *Phaeocystis* spp. overwhelmingly dominated the prymnesiophyte biomass during the SW Monsoon, we determined the relationship between PHAEO carbon biomass and the group-specific pigment 19′-hexanoylfucoxanthin (HEX) [PHAEO in μg $C\,l^{-1} = -2.3 + 0.06$(HEX in ng l^{-1}); $r = 0.68$; $n = 12$] and applied that to SW Monsoon stations lacking direct microscopical assessments. In contrast, *Phaeocystis* spp. were scarce during the NE Monsoon and the majority of the prymnesiophyte biomass was comprised of other genera. For this reason, we assumed that HEX concentrations during the NE Monsoon represent prymnesiophytes other than PHAEO, with coccolithophorids being the most common. Production due to PHAEO was greatest along the southern transect during the SW Monsoon (Fig. 4), with an excess of production over grazing at most stations. Despite the high biomass of PHAEO at N4, growth rates were low and indicated little production. Daily production attributed to PHAEO during the SW Monsoon ranged from 1% to 38%, (mean $= 10\%$) with a maximum at station S11 (Table 5). During the NE Monsoon, prymnesiophyte production increased somewhat on the northern transect and decreased in the south. Based on mean production and grazing estimates for all stations, grazing losses accounted for 100% of prymnesiophyte (namely PHAEO) production in the SW Monsoon and 65% during the NE Monsoon, with larger imbalances more notable on the southern transects of both cruises (Fig. 4).

Picoeukaryote biomass (PICO), estimated from the difference between FCM and microscopy, ranged from 1.3 to 28.6 μg $C\,l^{-1}$ and was highest at inshore stations (Table 3). PICO accounted for $\sim 43\%$ of autotrophic carbon during the NE Monsoon and ranged broadly from 5% to 67% of biomass during the SW Monsoon. The highest absolute and relative biomass contributions of PICO were at station N2 during the SW Monsoon (28.6 μg $C\,l^{-1}$).

3.5. Heterotrophic biomass and production

Biomass of mixed-layer heterotrophic bacteria (HBact) was similar between the two cruises, averaging 14 and 12 μg $C\,l^{-1}$ for the SW Monsoon and NE Monsoon, respectively. Bacterial biomass

Fig. 3. Spatial distribution of *Prochlorococcus* spp. and *Synechococcus* spp. production (*P*) rates and grazing losses to protists (*G*) from dilution experiments in the surface mixed layer. PRO production is estimated from FCM-measured changes in *Prochlorococcus* spp. cell abundance, SYN production is estimated from FCM-measured changes in *Synechococcus* spp. cell abundance and DIVA production is estimated from HPLC-measured changes in divinyl chlorophyll *a*.

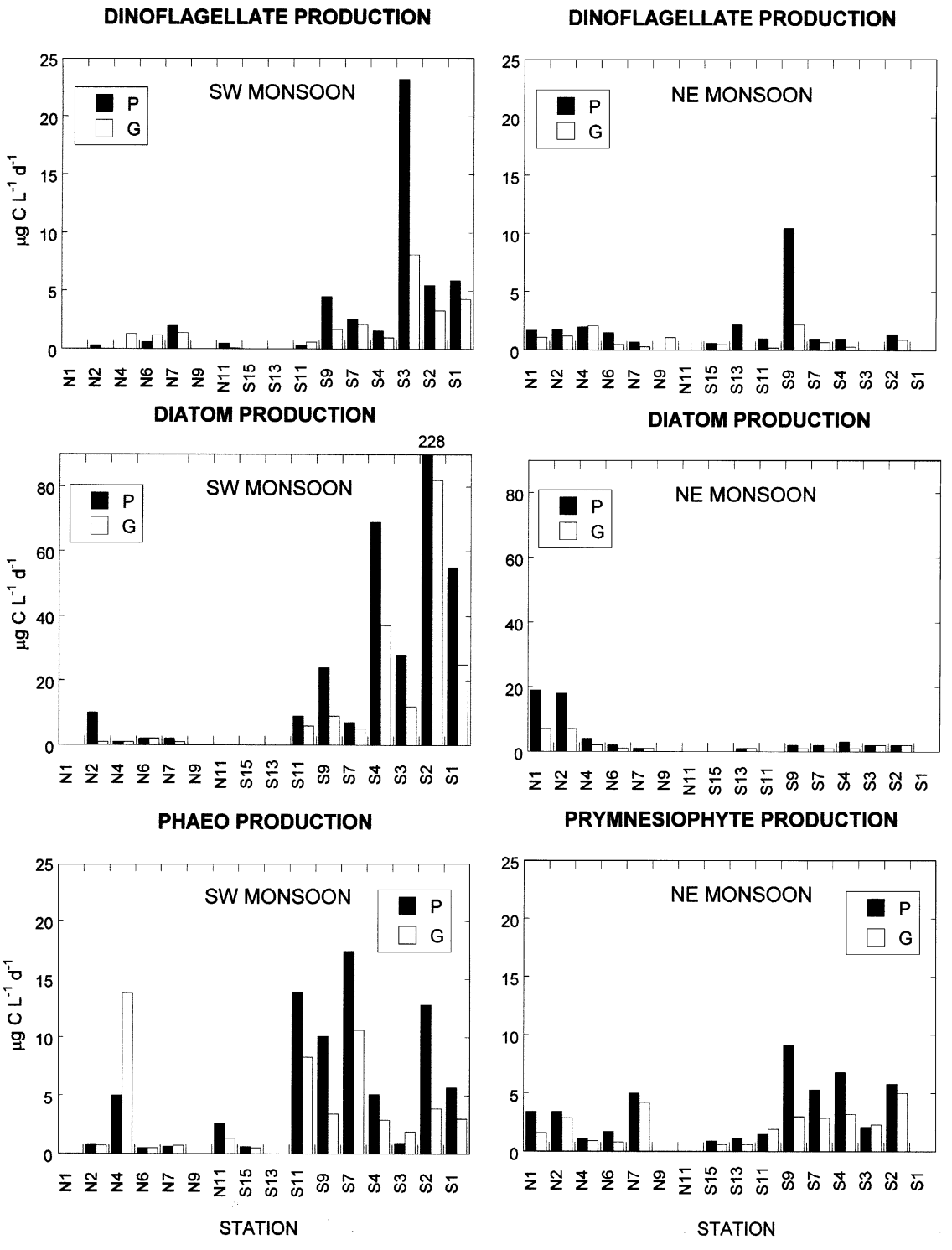
DINOFLAGELLATE PRODUCTION
SW MONSOON
NE MONSOON
DIATOM PRODUCTION
228
PHAEO PRODUCTION
PRYMNESIOPHYTE PRODUCTION
P
G
µg C L-1 d-1
STATION
N1 N2 N4 N6 N7 N9 N11 S15 S13 S11 S9 S7 S4 S3 S2 S1

Table 5
Biomass and production estimates averaged over the mixed layer for three major eukaryotic groups of phytoplankton

Cruise	STA	PDINO				DIAT				PHAEO/PRYM			
		P	%TP	*G*	*G*/*P*	*P*	%TP	*G*	*G*/*P*	*P*	%TP	*G*	*G*/*P*
SWM	**N2**	**0**	0	**0**	**0.06**	**12**	16	**1**	**0.07**	**1**	1	**1**	**0.83**
SWM	**N4**	**0**	0	**1**	**1.00**	**1**	1	**1**	**0.83**	**5**	0	**13**	**3.43**
SWM	N6	1	3	1	1.97	2	12	2	0.68	0	2	1	1.07
SWM	**N7**	**2**	7	**1**	**0.67**	**2**	7	**1**	**0.39**	**1**	2	**1**	**1.09**
SWM	**N11**	**0**	3	**0**	**0.31**	**0**	2	**0**	**0.35**	**3**	16	**1**	**0.50**
SWM	**S15**	**0**	0	**0**	—	**0**	1	**0**	**0.26**	**1**	8	**1**	**0.91**
SWM	**S11**	**0**	1	**1**	**1.69**	**11**	31	**7**	**0.61**	**14**	38	**8**	**0.60**
SWM	**S9**	**5**	4	**2**	**0.37**	**38**	33	**11**	**0.30**	**10**	9	**3**	**0.34**
SWM	**S7**	**3**	2	**2**	**0.79**	**14**	13	**7**	**0.48**	**17**	16	**11**	**0.61**
SWM	**S4**	**2**	1	**1**	**0.65**	**69**	53	**37**	**0.54**	**5**	4	**3**	**0.58**
SWM	**S3**	**23**	46	**8**	**0.35**	**28**	56	**12**	**0.42**	**1**	2	**2**	**2.24**
SWM	**S2**	**6**	3	**3**	**0.59**	**234**	114	**83**	**0.36**	**13**	6	**4**	**0.30**
SWM	**S1**	**6**	4	**4**	**0.74**	**60**	37	**26**	**0.44**	**6**	4	**3**	**0.52**
NEM	N1	3	2	1	0.44	34	31	9	0.26	5	4	2	0.34
NEM	N2	2	2	1	0.64	22	29	8	0.36	3	4	3	0.86
NEM	N4	2	6	2	1.03	4	12	2	0.40	1	3	1	0.81
NEM	N6	1	3	1	0.37	4	7	1	0.23	2	3	1	0.47
NEM	**N7**	**1**	1	**0**	**0.52**	**2**	3	**2**	**0.83**	5	6	4	0.85
NEM	N9	0	0	1	1.00	1	23	0	0.26	0	0	0	0
NEM	N11	0	0	1	1.00	0	3	0	2.79	0	0	0	0
NEM	**S15**	**1**	5	**1**	**0.81**	**0**	1	**0**	**0.47**	1	7	1	0.66
NEM	S13	2	9	0	0	3	14	1	0.36	1	4	1	0.59
NEM	**S11**	**1**	3	**0**	**0.21**	**1**	2	**1**	**0.71**	1	5	2	1.32
NEM	S9	11	15	2	0.21	5	8	2	0.31	9	13	3	0.33
NEM	**S7**	**1**	1	**1**	**0.69**	**3**	4	**1**	**0.33**	5	7	3	0.55
NEM	**S4**	**1**	2	**0**	**0.32**	**4**	7	**1**	**0.35**	7	11	3	0.47
NEM	S3	0	0	0	—	3	13	2	0.78	2	10	2	1.08
NEM	**S2**	**1**	4	**1**	**0.67**	**3**	10	**2**	**0.59**	6	17	5	0.87

SWM = Southwest Monsoon (TN050), NEM = Northeast Monsoon (TN054). PDINO = photosynthetic dinoflagellates, DIAT = diatoms, PHAEO = *Phaeocystis* spp. during SWM, and PRYM = prymnesiophytes during NEM. *P* and *G* are daily production rates and losses due to microzooplankton grazing (μg $C l^{-1} d^{-1}$), respectively. %TP is the percent of total phytoplankton production attributed to each group. Production and loss rates for the three groups are based on peridinin, fucoxanthin and 19′-hexanoylfucoxanthin synthesis and loss rates. *G*/*P* represents the ratio of grazing losses to daily production. Stations in bold denote measured biomass; at other stations, biomass is derived from carbon to pigment relationships as described in text.

was more or less uniformly distributed during the SW Monsoon, with an area of low biomass at the offshore station S15. During the NE Monsoon, biomass followed an onshore to offshore gradient along both transects, with highest levels (31 μg $C l^{-1}$) along the northern transect (Table 6). Despite the seasonal similarity in standing stock, rate estimates for production and grazing differed substantially (Fig. 5). Production averaged 17 μg $C l^{-1} d^{-1}$ during the SW Monsoon, ranging from 1.1 μg $C l^{-1} d^{-1}$ at station S15 to 35.1 μg $C l^{-1} d^{-1}$ adjacent to the coast. In contrast, bacterial

Fig. 4. Spatial distribution of daily production (*P*) rates and grazing losses to protists (*G*) for three eukaryotic groups. Rate estimates are from dilution experiments in the surface mixed layer. Dinoflagellate estimates are from changes in peridinin concentrations; diatom estimates are from changes in fucoxanthin concentrations. *Phaeocystis* spp. (PHAEO) estimates are from 19′-hexanoyloxyfucoxanthin during the SW Monsoon season; during the NE Monsoon, rate estimates include all prymnesiophytes (PRYM). Note the scale change in the *y*-axis.

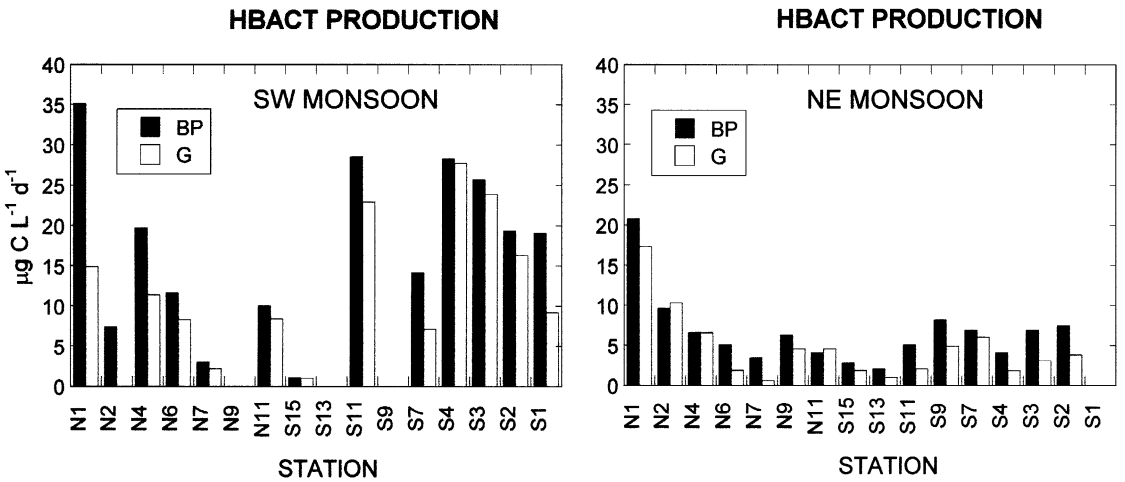

Fig. 5. Spatial distributions of daily heterotrophic bacteria production (BP) rates and grazing losses to protists (*G*) from dilution experiments in the surface mixed layer. Rates are determined from FCM-measured changes in the heterotrophic bacteria community.

production averaged only 7 μg $C l^{-1} d^{-1}$ (range = 2.1–20.8 μg $C l^{-1} d^{-1}$) during the NE Monsoon. Grazing estimates scaled accordingly, with mean loss rates of 12 μg $C l^{-1} d^{-1}$ during the SW Monsoon and 5 μg $C l^{-1} d^{-1}$ during the NE Monsoon. Accordingly, the average percentages of bacterial production lost to grazing (66%) for both cruises, and net production (*P–G*) (2.6 and 2.0 μg $C l^{-1} d^{-1}$, respectively) were similar for both cruises. Bacterial production estimates were 36% of primary production over both cruises, averaging 57% of primary production during the SW Monsoon and 17% during the NE Monsoon.

Total micrograzer biomass (2–200 μm) in the mixed-layer ranged an order of magnitude from 1.1 to 12.2 μg $C l^{-1}$ and did not appear to follow a discernable spatial pattern (Table 6). Heterotrophic flagellates, dinoflagellates and ciliates showed similar levels of biomass, although at different stations. The size distributions of grazers also varied spatially. For example, the average size of ciliates was greater than that of heterotrophic dinoflagellates at stations S1 and S15 during the SW Monsoon, but was smaller at station S11 where large thecate dinoflagellates dominated the grazer biomass (see Garrison et al., 1998, Figs. 5–7). Estimates of grazer biomass are only available for six stations during the NE Monsoon. Although the range of biomass was less (4–8 μg $C l^{-1}$) and the mean was the same as for the SW Monsoon (6 μg $C l^{-1}$), grazer biomass was not measured at the higher chlorophyll *a*, northern coastal stations with high grazing on HBact (Table 6). Heterotrophic dinoflagellates dominated the biomass at the six stations sampled during the NE Monsoon. Total heterotrophic carbon (HC) ranged from 7 to 28.4 μg $C l^{-1}$ and was always dominated by HBact (Table 6).

4. Discussion

4.1. Phytoplankton production

Production rates from dilution experiments are based on three measured terms—growth and grazing rates and assessments of initial biomass. Taxon-specific production estimates are further complicated by the use of different diagnostic pigments for characterizing rates and different approaches (flow cytometry, microscopy, pigment:biomass ratios) for quantifying biomass. Despite these complications, the sum of production and grazing estimates for major taxa (PRO, SYN, DINO, DIAT, PHAEO/PRYM) were generally in good agreement with the total community estimates based on chlorophyll *a* (Fig. 6). Consequently, we can assume that we have identified and

Table 6
Biomass and production estimates for heterotrophic bacteria (HBact) and protistan grazers in the mixed layer

Cruise	STA	Hbact				HF	HD	CIL	TIN	GC	HC
		B_0	BP	G	G/BP						
SWM	N1	19.2	35.1	14.9	0.42	—	—	—	—	—	—
SWM	N2	15.6	7.4	0.0	0	0.3	0.5	0.3	0.0	1.1	16.7
SWM	N4	17.1	19.7	11.4	0.58	4.1	3.5	0.9	0.0	8.5	25.6
SWM	N6	11.2	11.6	8.3	0.71	—	—	—	—	—	—
SWM	N7	9.4	3.0	2.2	0.72	0.9	2.5	2.3	0.2	5.9	15.3
SWM	N11	10.4	10.0	8.4	0.84	1.1	2.3	0.8	0.0	4.2	14.6
SWM	S15	4.0	1.1	1.0	0.91	1.2	1.4	0.5	0.0	3.1	7.0
SWM	S11	19.3	28.5	22.9	0.80	1.8	3.5	1.8	0.0	7.1	26.4
SWM	S9	—	—	—	—	0.6	2.0	1.2	0.0	3.8	—
SWM	S7	13.3	14.2	7.2	0.51	1.9	2.2	2.6	1.3	8.0	21.3
SWM	S4	22.3	28.3	27.7	0.98	1.6	2.2	1.9	0.4	6.1	28.4
SWM	S3	17.4	25.7	23.9	0.93	1.2	2.8	0.0	0.0	4.0	21.5
SWM	S2	13.4	19.4	16.3	0.84	1.9	4.4	5.7	0.2	12.2	25.6
SWM	S1	12.9	19.1	9.2	0.48	2.2	1.9	2.4	0.0	6.5	19.4
NEM	N1	30.8	20.8	17.3	0.83	—	—	—	—	—	—
NEM	N2	24.6	9.6	10.3	1.08	—	—	—	—	—	—
NEM	N4	11.0	6.6	6.6	1.00	—	—	—	—	—	—
NEM	N6	8.1	5.1	1.9	0.38	—	—	—	—	—	—
NEM	N7	9.5	3.4	0.6	0.17	0.7	1.9	1.2	0.2	4.0	13.5
NEM	N9	7.6	6.3	4.6	0.72	—	—	—	—	—	—
NEM	N11	6.9	4.1	4.6	1.11	—	—	—	—	—	—
NEM	S15	7.8	2.8	1.9	0.69	0.5	1.8	1.2	0.9	4.4	12.2
NEM	S13	4.4	2.1	1.0	0.48	—	—	—	—	—	—
NEM	S11	8.3	5.1	2.1	0.42	0.4	3.8	1.2	0.1	5.5	13.8
NEM	S9	10.5	8.2	4.9	0.60	—	—	—	—	—	—
NEM	S7	13.6	6.9	6.0	0.87	1.2	3.5	2.7	0.2	7.6	21.2
NEM	S4	9.6	4.1	1.9	0.47	0.5	2.9	2.0	0.0	5.4	15.1
NEM	S3	9.5	6.9	3.1	0.44	—	—	—	—	—	—
NEM	S2	13.5	7.5	3.8	0.50	0.3	4.6	2.0	1.1	8.0	21.5

SWM = Southwest Monsoon (TN050), NEM = Northeast Monsoon (TN054). For HBact: B_0 = initial biomass in μg $C l^{-1}$, BP = bacterial production and G = production losses to grazing both in μg $C l^{-1} d^{-1}$; G/BP represents the ratio of grazing losses to daily bacterial production. HF, HD, CIL and TIN represent the biomass (μg $C l^{-1}$) of heterotrophic flagellates, heterotrophic dinoflagellates, ciliates and tintinnids respectively. GC is the total grazer carbon and HC is the total heterotrophic carbon, both in μg $C l^{-1}$.

quantified the major groups responsible for primary production at most stations and have accounted for most of their daily production losses to protistan grazing.

We saw a remarkable abundance of PEUKS at station N2 during the SW Monsoon ($\sim$90,000 cells ml^{-1}), coincident with the largest difference between FCM and microscopical estimates, suggesting that a substantial population of small cells was missed by microscopy. A similar, but less abundant population appeared to have been present at station S2. Closer inspection of FCM scattergrams revealed a distinct, dense population of small PEUKS with light-scattering properties indicating a cell size $\sim$1 μm in diameter and resembling the recently discovered smallest eukaryote *Ostreococcus tauri* (Courties et al., 1994, 1998; Chretiennot-Dinet et al., 1995). Pigment concentrations are also consistent with that of *O. tauri*, showing maxima of the characteristic pigments prasinoxanthin and violaxanthin at these stations (Chretiennot-Dinet et al., 1995; H. Claustre, pers. comm.). Because of its light-scattering properties and a reported cell size of

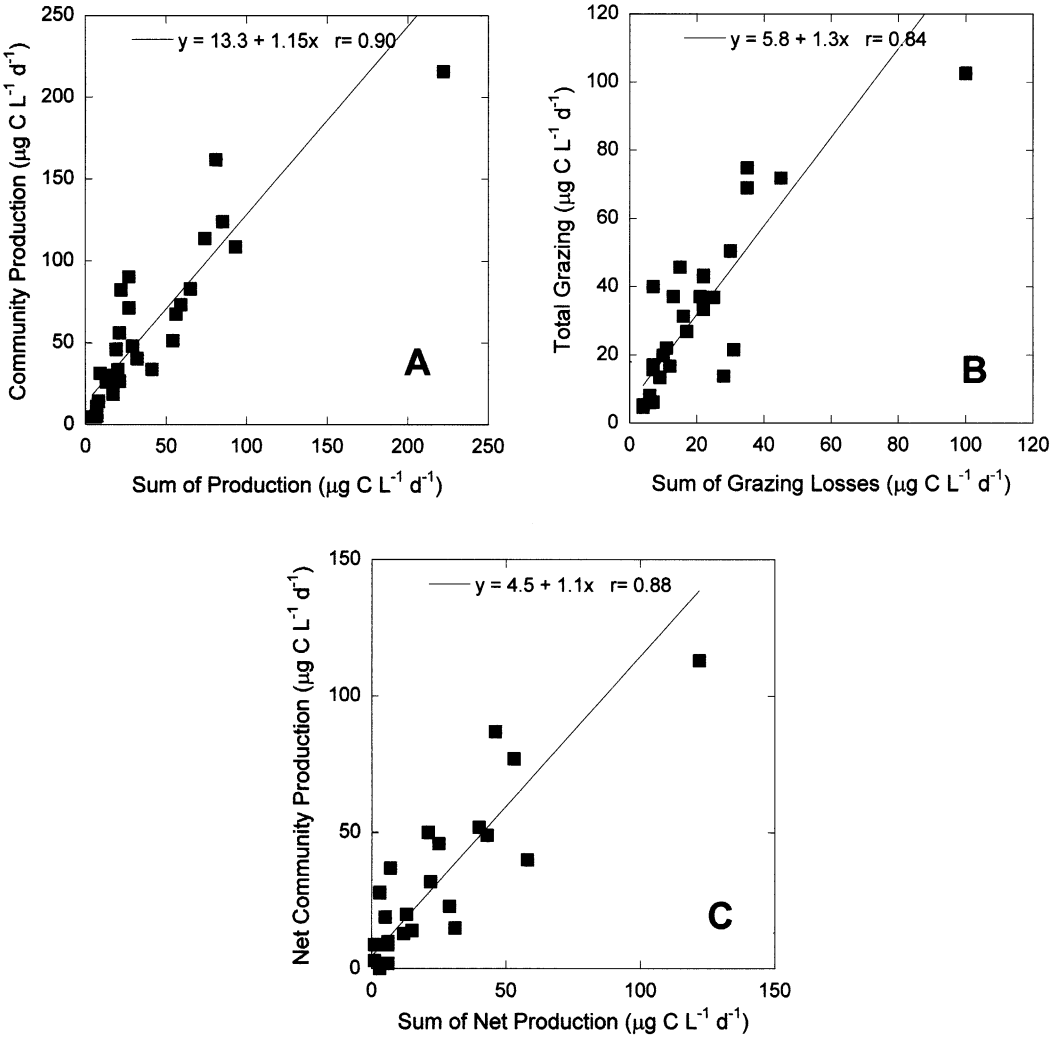

Fig. 6. Panel A shows the relationship between primary production estimates (PP) for the total phytoplankton community based on HPLC total chlorophyll *a* and the sum of individual group production estimates (PRO + SYN + DINO + DIAT + PHAEO/PRYM). Panel B shows the relationship between net production estimates (PP–*G*) for the total phytoplankton community based on HPLC total chlorophyll *a* and the sum of individual group production estimates. Panel C shows the relationship between grazing losses estimated for the total phytoplankton community based on HPLC total chlorophyll *a* and the sum of grazing losses for individual groups. Relationships are based on major axis Model II linear regressions, $n = 28$.

$0.97 \times 0.7\,\mu m$ for *O. tauri* (Courties et al., 1998), we applied a biomass conversion factor of 85 fg C cell^{-1} to these cells. Based on the deficit between total phytoplankton production (75 μg C l^{-1} d^{-1}) and that attributable to the major taxa (27 μg C l^{-1} d^{-1}), this population of small eukaryotes may have contributed up to 65% of primary production at station N2 in the SW Monsoon.

While the comparisons in Fig. 6 suggest our production estimates are at least internally consistent, uptake of ^{14}C provides an independent assessment of the magnitude of our results. There has been significant discussion in the literature regarding the distinction between gross and net photosynthesis and which parameter the incorporation of ^{14}C-labeled carbon represents. In a

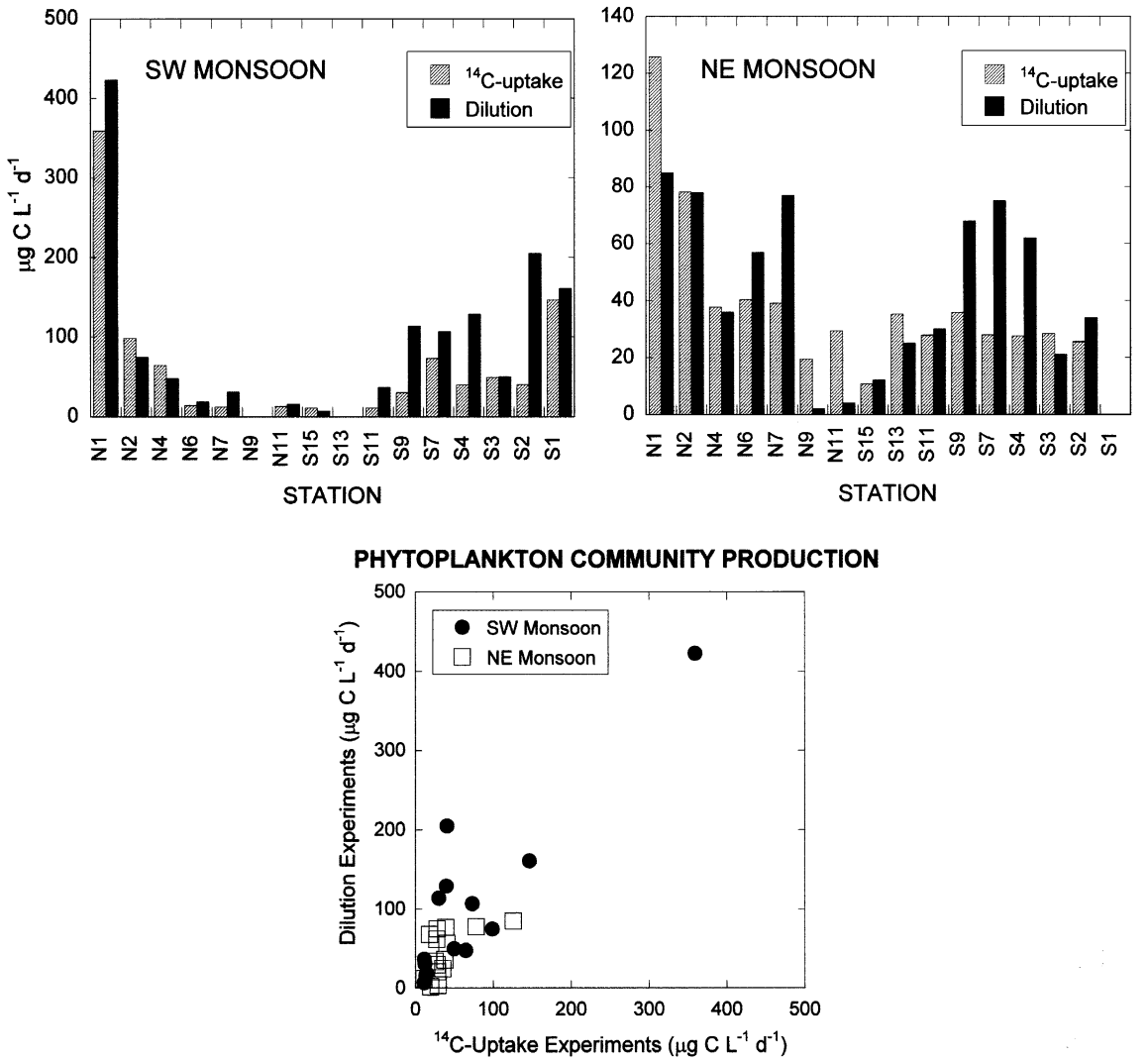

Fig. 7. Top two panels show total phytoplankton community production estimates from ^{14}C-uptake experiments and dilution experiments during the SW and NE Monsoon seasons. ^{14}C-uptake rates are integrated averages to depths corresponding to dilution experiments. Bottom panel shows a scatter plot of the same data from ^{14}C-uptake experiments and dilution experiments.

theoretical analysis of photosynthesis combined with field results from the Arabian Sea, Laws et al. (2000) concluded that ^{14}C-uptake represents 48% of gross carbon production (=Net+Respiration) and that grazing reduces the measured ^{14}C particulate carbon uptake by ~15%. From this, we would expect that measured rates of ^{14}C-uptake would equal about 85% of the autotrophic growth of phytoplankton as measured from dilution experiments.

Production estimates from mixed-layer dilution experiments and those from ^{14}C-uptake incubations at comparable light levels showed similar spatial trends and were close in magnitude for the SW Monsoon, with ^{14}C-uptake estimates averaging 76% of dilution estimates (Fig. 7). During the NE Monsoon, however, the comparison was less satisfying, particularly at offshore stations N9 and N11. The mean ^{14}C-based estimate for this cruise was 90% of the dilution mean, the

difference from theory suggesting slight underestimates of dilution rates overall. Spatially, ^{14}C-uptake rates were remarkably constant along the southern line during the NE Monsoon, while dilution estimates indicated more of a spatial gradient, seemingly corresponding to nitrate concentrations (Table 1). Potential causes of the methodological discrepancies on the NE Monsoon cruise are (1) imprecise estimates of phytoplankton biomass, (2) variability due to mesoscale physical processes, and (3) uncoupling between estimates of pigment synthesis and phytoplankton cell growth and/or pigment destruction and protistan grazing.

Station-specific biomass was only available for six of the stations during the NE Monsoon, and C:Chl *a* ratios were used to infer biomass at the remaining stations. Since the ratios used were relatively low compared to recent estimates from the equatorial Pacific Ocean under similar hydrographic conditions (Chavez et al., 1996; Brown et al., in review), biomass may have been systematically underestimated, particularly at offshore stations. Further uncertainty in biomass estimates may be attributed to the difference between phytoplankton abundances from FCM and microscopy, attributed here mostly to eukaryotes $\leqslant 2.5\,\mu m$ in diameter.

Regarding spatial variability, we note that water for biomass estimates, ^{14}C-experiments, and dilution rate estimates was taken from different hydrographic casts. These casts were generally close in time (<24 h); however, biomass and HPLC pigment estimates from multiple casts at a given station did differ substantially at times. For example, in different bottle samples at station S9 during the SW Monsoon, diatom biomass varied from 3 to 18 $\mu g\,C\,l^{-1}$. Given that small spatial and short time-scale hydrographic variability exceeded seasonal signals (Kim et al., 2001) due to the dominance of mesoscale squirts, eddies and filaments (Brink et al., 1996; Dickey et al., 1998; Manghnani et al., 1998; Flagg and Kim, 1998), significant differences in initial biomass could explain much of the disparity in production estimates. However, production estimates differed more during the NE Monsoon when conditions were more static and there was less hydrographic variability.

We have tried to account for an uncoupling between pigment synthesis and phytoplankton growth by correcting pigment-based growth estimates for photoadaptive changes in cellular fluorescence as inferred from FCM. While grazing estimates should not be affected by pigment photoadaptation (Landry et al., 2002), it is possible that pigment-based grazing rates may have been underestimated if experiments were terminated after dark and some portion of grazed pigments were not degraded (Klein et al., 1986; Strom, 1993; Landry et al., submitted). To minimize this problem, the majority of our experiments began and ended in the late afternoon. Nevertheless, we can assess potential uncoupling by comparing production and grazing losses from FCM-PEUKS with those from HPLC measured monovinyl chlorophyll *a* (Chl *a*). Based on Model II linear regressions [(major axis) [Chl *a* in $ng\,l^{-1} = 9 + 0.99$ PEUKS in cells ml^{-1} ($r = 0.90$, $n = 29$) for losses due to grazing and Chl *a* in $ng\,l^{-1} = 13 + 0.95$ PEUKS in cells ml^{-1} ($r = 0.93$, $n = 29$) for daily production estimates], an uncoupling between pigments and biomass did not appear to occur.

It should be noted that our daily primary production calculations differ from the previous equation of Vaulot et al. (1995) [$PP = C_0(e^{\mu} - 1)$, where C_0 is the initial phytoplankton biomass] used in Brown et al. (1999) and Liu et al. (1998), which does not account for grazing losses over a 24-h period. The present production estimates take into account that the average concentration of phytoplankton (C_m) producing carbon over a 24-h incubation is not the same as the initial carbon concentration (C_0), due to grazing losses (Laws et al., 1984); this is an important distinction in the estimation of production. This difference, along with higher carbon per cell conversion factors, explains the much higher estimates of prokaryote production previously reported for Arabian Sea populations by Liu et al. (1998) and Brown et al. (1999).

4.2. Bacterial secondary production

FCM analyses of dilution experiments allow for rapid and precise quantification of changes in

heterotrophic bacterial populations. Bacterial rate estimates must be viewed with caution, however, as it is not clear how well the critical assumptions of the dilution technique apply to heterotrophic growth. Of primary concern is the assumption that growth rates are constant and unaffected by dilution (Landry and Hassett, 1982). While the growth of autotrophs can be kept constant by the addition of saturating levels of potentially limiting inorganic nutrients, the availability of organic substrates for bacterial growth is an uncontrolled parameter. Carbon enrichment from lytic release during filtration (Ferguson et al., 1984) could exaggerate the growth of bacterial cells, as could reduced competition for available carbon sources in the more dilute treatments. In previous studies, carbon enrichment effects have been shown to be negligible (Tremaine and Mills, 1987). This also could be the case in the Arabian Sea because it appears to be characterized by year round, unusually constant levels of excess labile and/or semi-labile DOC (Carlson and Ducklow, 1995; Ducklow et al., 2001).

Bacterial production during the NE Monsoon was estimated by ^{3}H-leucine and -thymidine incorporation (http://www1.whoi.edu/jg/dir/jgofs/arabian/ttn-054), allowing a direct comparison with our dilution estimates. Incorporation of ^{3}H-leucine during protein synthesis represents bacterial biomass growth, while the ^{3}H-thymidine incorporation during DNA synthesis reflects cell division or reproduction (Shiah and Ducklow, 1997). Comparing the results from 0.5 to 2-h dark incubations averaged over corresponding depth strata to our cell-based production, dilution estimates were more closely correlated with incorporation of ^{3}H-leucine ($r = 0.75$, $n = 14$) and showed similar spatial trends (Fig. 8). Such a comparison is complicated by the distinction between net and gross production and which parameter is measured by ^{3}H-leucine uptake. Production estimates from ^{3}H-leucine fell within our estimates of gross (BP) and net (BP$-G$) bacterial production for the NE Monsoon (Fig. 8); on average, gross bacterial production estimates from dilution experiments were 1.7-fold greater than ^{3}H-leucine production estimates. The lower rate estimates from ^{3}H-leucine uptake could

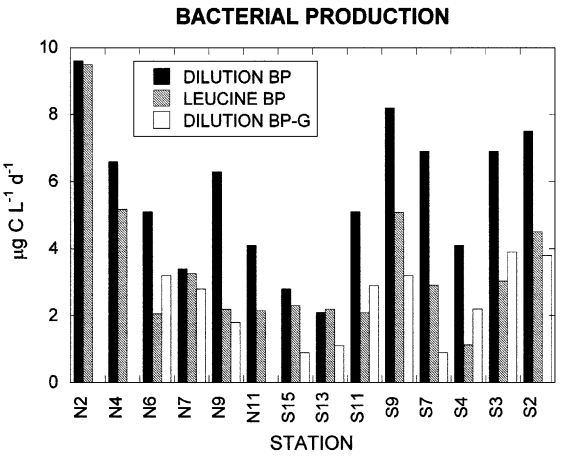

Fig. 8. Gross and net (BP–G) bacterial production estimates from dilution experiments and uptake of ^{3}H-leucine during the NE Monsoon.

suggest that the method represents production that lies somewhere between net and gross. Alternatively, the lower rate estimates from ^{3}H-leucine uptake could be attributed to an extracellular or intracellular isotopic dilution effect, a potential problem with both thymidine and leucine methods (Karl, 1986).

Since the incorporation of ^{3}H-leucine was not measured during the late SW Monsoon, dilution estimates of net and gross bacterial production provide a range within which we would expect those rates to lie. The observed difference between dilution production estimates for the two seasons (SW Monsoon $\sim$2.4-fold greater than the NE Monsoon) is consistent with the conclusion by Ducklow et al. (2001) that bacterial production only increased by a factor of two during the early SW Monsoon season. In addition, the similarity in average net production rates between the two seasons (2.6 and 2.0 µg C l^{-1} d^{-1}) may explain the observed constancy of biomass.

4.3. Physical forcing

Landry et al. (1998) showed that growth rate of the Arabian Sea phytoplankton community varied with nitrate concentration. However, individual taxa showed different growth responses to

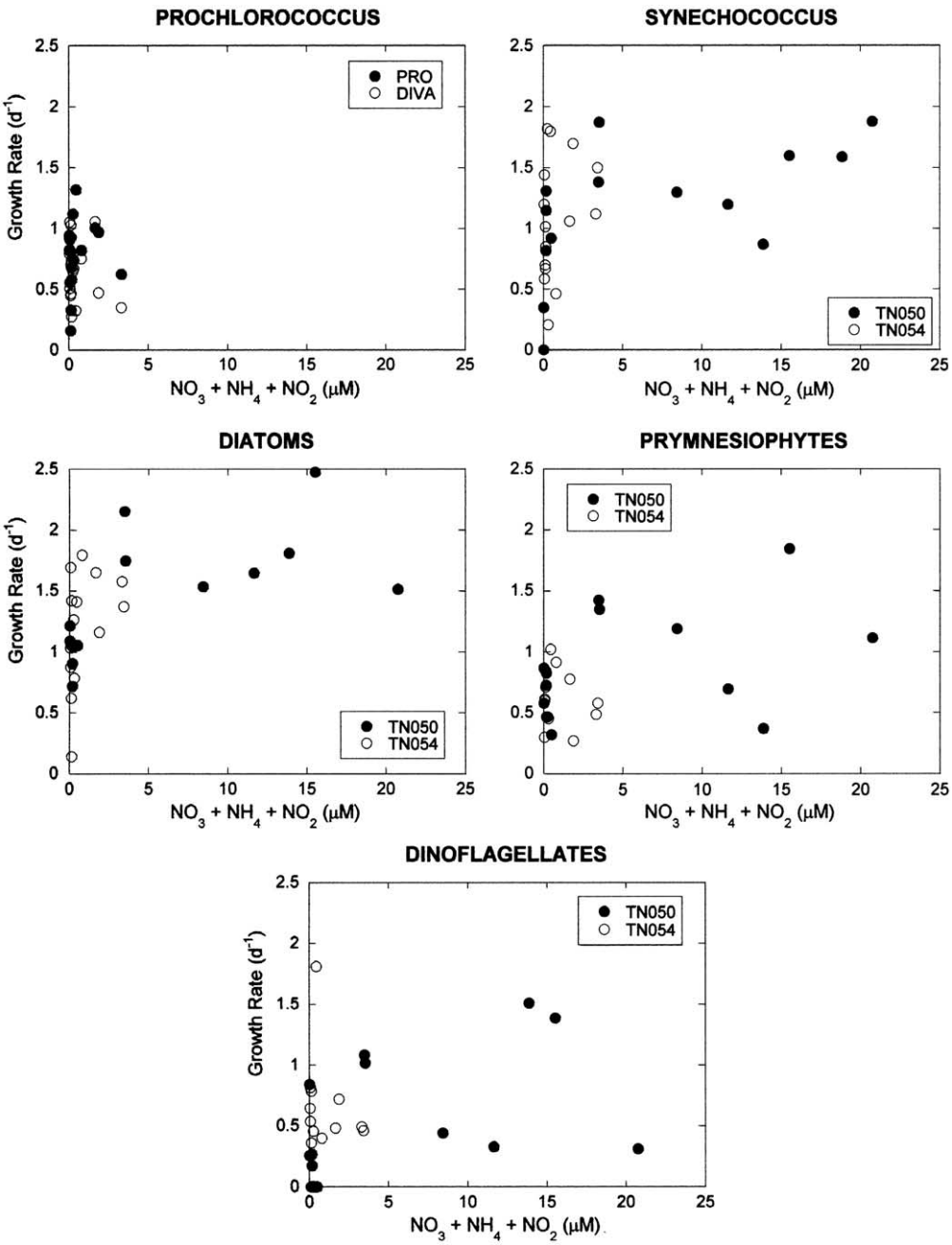

Fig. 9. Growth rate estimates as a function of dissolved inorganic nitrogen. Growth rates for dinoflagellates, diatoms and prymnesiophytes were derived from changes in peridinin, fucoxanthin, and 19′-hexanoyloxyfucoxanthin, respectively. Growth rates estimated for *Prochlorococcus* and *Synechococcus* spp. were derived from FCM. DIVA = divinyl chlorophyll *a*.

increasing nutrients. *Prochlorococcus* spp. growth showed no relationship to dissolved inorganic nitrogen (Fig. 9); however, cell abundances were negligible at high nitrate concentrations, which is consistent with reports from previous studies off the coast of Oman (Tarran et al., 1999).

Despite variability at nitrate concentrations $>5\,\mu M$, *Synechococcus* spp. growth rates generally appeared to increase with increasing nitrogen concentrations, particularly during the SW Monsoon (Fig. 9). Individual growth rate estimates were as high as $2.0\,d^{-1}$ and mean rate estimates at concentrations above $1\,\mu M$ NO_3 averaged $1.5\,d^{-1}$. Diatoms exhibited the most definitive relationship of increasing growth as a function of nitrogen concentrations. At nitrogen concentrations $>3.5\,\mu m$, growth rates exceeded $1.5\,d^{-1}$, over two doublings per day. In contrast, neither prymnesiophytes nor dinoflagellates exhibited strong growth rate responses to enhanced nitrogen concentrations, and mean growth rates at high nutrient concentrations were substantially less than those of *Synechococcus* spp. and diatoms. During the SW Monsoon, prymnesiophytes were comprised primarily of *Phaeocystis* spp. The complex life cycle of *Phaeocystis* spp., and temporal succession following the exhaustion of nutrients by diatoms (Latasa and Bidigare, 1998), may explain the lack of a clear relationship between growth and nitrogen during this time. Given the sensitivity of dinoflagellates to turbulence (Thomas and Gibson, 1990), optimal growth conditions may be in an intermediate region of a stratified water column with sufficient nutrients for growth. In fact, highest growth rates were at the intermediate station S9 during both seasons and following relaxation of monsoonal winds at S2 and S3.

4.4. Grazing relationships

Spatial variability in hydrography, phytoplankton abundance, and community structure makes the unraveling of grazer interactions difficult. With the exception of station N7 during the NE Monsoon, grazing rates were reasonably well correlated with grazer biomass over both seasons (Fig. 10). The high grazing rate at station N7, despite modest grazer biomass, reflects high phytoplankton community growth rates ($\mu = 2.1\,d^{-1}$) and the close coupling between growth and mortality rates offshore. Carbon consumption by protists (G) increased linearly with phytoplankton carbon, implying that protistan grazing was not saturated even at the highest levels of phytoplankton biomass (Fig. 10). Despite high grazing rates and seemingly sufficient prey levels, the biomass of grazers was quite modest (1–30% of phytoplankton carbon) across the region during both seasons. In addition, grazer biomass was similar between seasons, despite a factor of two difference in phytoplankton biomass. Such consistently low and constant protistan biomass suggests top-down control by a higher

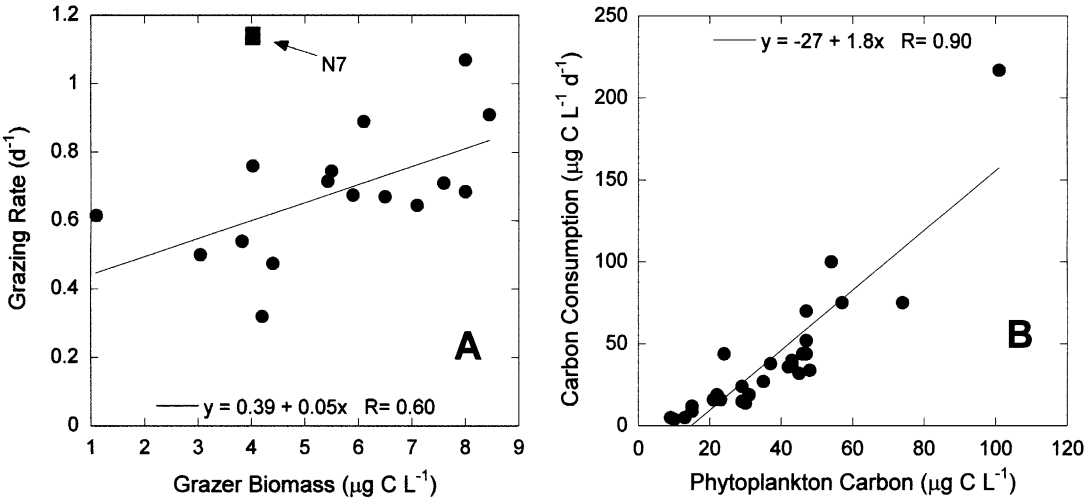

Fig. 10. Relationship between grazer biomass (µg $C\,l^{-1}$) and grazing rates (d^{-1}) (Panel A) and phytoplankton carbon (µg $C\,l^{-1}$) and protistan carbon consumption (µg $C\,l^{-1}\,d^{-1}$) (Panel B).

trophic level (Stelfox et al., 1999), presumably crustacean mesozooplankton, which were present in high abundances (Smith et al., 1998b). Protists often comprise a substantial portion of the mesozooplankton diet (Stoecker and Capuzzo, 1990; Gifford and Dagg, 1991; Kleppel, 1992; Dam et al., 1995; Verity and Paffenhoffer, 1996; Roman and Gauzens, 1997), and at least 20% of mesozooplankton carbon consumption in the Arabian Sea may be attributable to protists (Roman et al., 2000).

Carbon-specific grazing estimates show that heterotrophic protists consumed a minimum of 2 to 36 times their body C d^{-1}, exclusive of predator-prey interactions among themselves (Fig. 11). Assuming a gross growth efficiency of 30%, protistan growth based on ingestion of phytoplankton and heterotrophic bacteria ranged from 0.5 to 2.5 d^{-1}. The unusually high carbon-specific grazing rate at station N2 reflects low grazer biomass. As this station was dominated by tiny PICOS missed by microscopy, it follows that a correspondingly small population of flagellated grazers also may have been present and unaccounted for by our methods. From this rough calculation, it appears that protists were turning over more slowly at the offshore stations, which is intuitively reasonable. However, protistan carbon demands at these stations also may have been supplemented by mixotrophy, which is suggested to be common in similar oligotrophic waters (Constantinou, 1994; Landry and Kirchman, 2002). Although difficult to quantify, mixotrophic ciliates and dinoflagellates appeared to have been ubiquitous in both nanoplankton and microplankton size fractions (Garrison et al., 1998).

Similar growth inferences can be made for heterotrophic flagellates (HFLAG), the primary grazers of prokaryotic prey: *Prochlorococcus* spp., *Synechococcus* spp. and heterotrophic bacteria. If we assume that essentially all of the grazing losses (G) for these groups were attributed to HFLAG, we calculate a somewhat constant growth rate average for HFLAG of 1.6 d^{-1}, with the exception of station N4 during the SW Monsoon (growth = 0.74 d^{-1}). The relatively constant growth rate of HFLAG, despite dramatic variations in the relative proportions of PRO, SYN and HBact, presumably reflects their ability to feed on any and all of the three picoplankton groups. These growth rate inferences for HFLAG should be viewed as conservative as we have not taken into account consumption of similarly sized picoeukaryotes, which were abundant at coastal upwelling stations (Table 3) (Latasa and Bidigare, 1998; Shalapyonok et al., 2001).

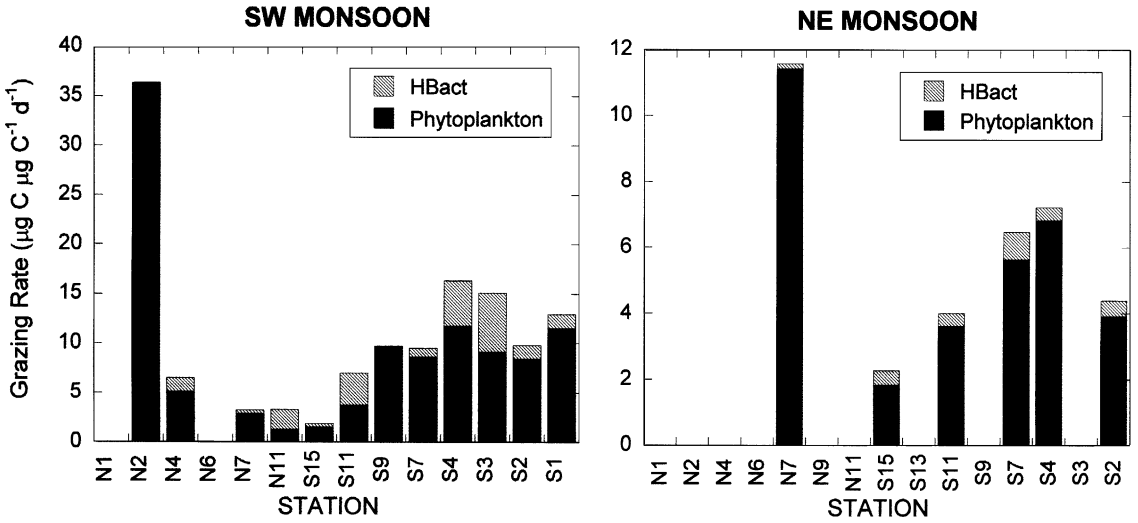

Fig. 11. Spatial distribution of biomass-specific grazing rates (µg C µg C d^{-1}).

Theoretical predictions of prey vulnerability to direct interception feeding by flagellates suggest that rates of mortality for HBact, PRO, and SYN should be linked to prey size (Fenchel, 1982, 1984; Gonzales et al., 1990; Monger and Landry, 1990, 1991). The models differ, however, in the predicted relationship between clearance rates and prey diameter, ranging from increasing with the first power to the third power of prey diameter. Taking into consideration average mortality rates during the NE Monsoon, when PRO was sufficiently abundant and rates were measurable from FCM, mortality rates were 0.35, 0.56 and $0.66\,d^{-1}$ for HBact, PRO and SYN, respectively. Assuming average diameters of 0.40, 0.64, and 0.95 μm for HBact, PRO and SYN, respectively, (Shalapyonok et al., 2001; Ducklow et al., 2001), mortality rates correspond most closely to the first power of prey diameter, consistent with the Force-Balance model of Monger and Landry (1990, 1991).

Group-specific relationships between grazers and phytoplankton prey are confounded by variations in size within prey types (e.g., diatoms) and within general groups of grazers. There was no clear relationship between diatom mortality (inferred from fucoxanthin) and either ciliates or heterotrophic dinoflagellates. This is likely due to spatial differences in the size spectra of diatom communities that dictate grazer pathways. For example, diatom biomass at station S11 during the SW Monsoon was dominated by centric diatoms and other large genera, such as *Rhizosolenia* and *Thassiothrix*, that are more likely to be grazed by large heterotrophic dinoflagellates if at all, while station S1 was dominated by smaller pennate diatoms that can be grazed effectively by larger protists (Landry et al., 2000). Similar complications arise with grazing rates on *Phaeocystis* spp., which existed both as solitary motile cells ($\sim 3\,\mu m$ diameter) and as macroscopic colonies. However, total grazer biomass was significantly correlated ($n = 18$) with mortality rates (g) of diatoms ($r = 0.49$) and dinoflagellates ($r = 0.48$), as well as with chlorophyll c ($r = 0.48$), the latter a broad-spectrum marker for eukaryotic phytoplankton, indicating a general grazer response to shifts in community structure. In general, diatoms were grazed the least effectively, with only 50% of daily production lost to protistan grazing, versus 66% and 80% for dinoflagellates and *Phaeocystis* spp., respectively.

Adaptations of the grazing community to shifts in phytoplankton community structure also can be seen in the sources of carbon passing through protistan grazers. During the SW Monsoon, much of the carbon grazed along the southern line came from major eukaryotic taxa of phytoplankton (diatoms, dinoflagellates and *Phaeocystis* spp.), reflecting the dominance of eukaryotic phytoplankton and adaptive response of protists to larger prey, and suggesting fewer trophic steps within the microbial community (Fig. 12). However, the fraction of grazed carbon attributed to eukaryotic taxa was substantially less than the eukaryote contribution to total biomass during the NE Monsoon (Fig. 13), indicating an inability of the protistan community to graze these taxa effectively. In contrast, photosynthetic prokaryotes were grazed in greater proportion than the fraction of biomass that they represented, demonstrating the ability of protists to respond to and graze smaller prey.

The majority of the carbon passing through protists during the NE Monsoon was attributed to prokaryotic picoplankton (Fig. 12), suggesting significant grazing pressure by small heterotrophic flagellates and thus more steps and greater remineralization within the microbial community. These two contrasting grazing pathways are consistent with conceptual models of Garrison et al. (2000) and provide further evidence for variations in carbon cycling efficiency within the microbial community.

4.5. Fate of ungrazed production

With respect to particulate flux, we are most interested in the fraction of production ungrazed by protists since this remains potentially available for export via mesozooplankton grazing pathways, lateral advection, and/or sinking. During the late SW Monsoon, 50% of mixed-layer primary production remained ungrazed at upwelling-influenced stations along the southern transect and northern coastal stations, while $<30\%$ remained ungrazed offshore. During the early NE Monsoon,

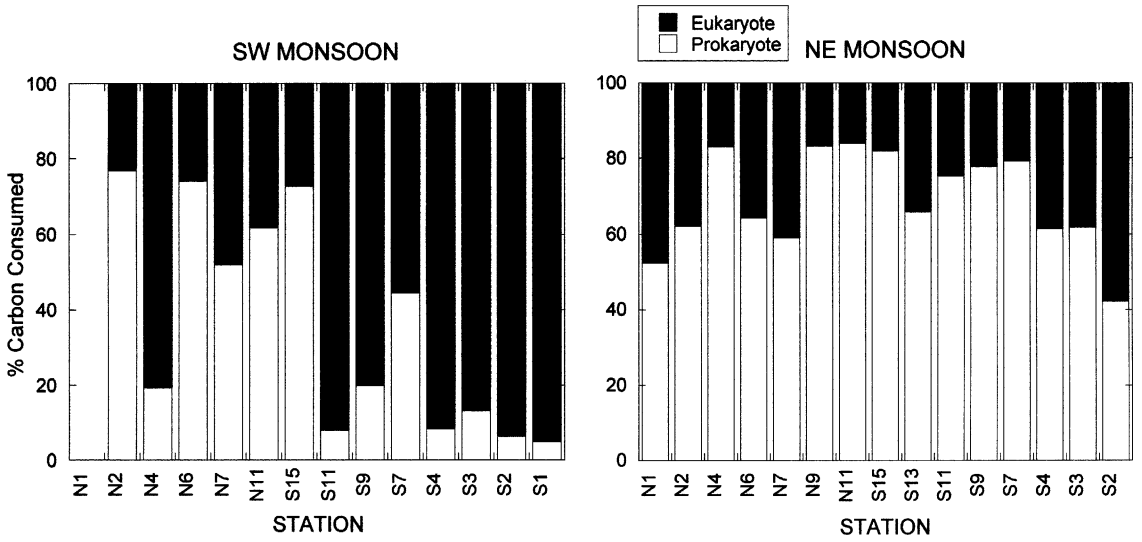

Fig. 12. The proportion of carbon grazed by protists that is attributed to prokaryotic and eukaryotic taxa.

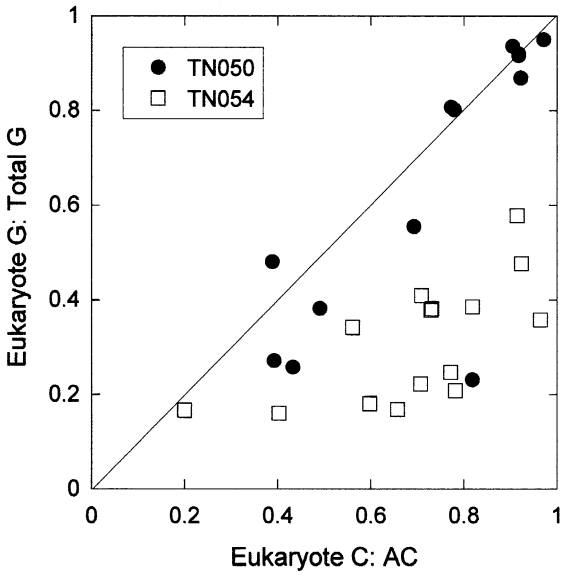

Fig. 13. The fraction of eukaryote biomass relative to total phytoplankton biomass versus the fraction of eukaryote biomass grazed. Line indicates a 1:1 relationship.

estimates ranged broadly from balanced production and microbial grazing offshore to >50% ungrazed production along the northern transect. Of the daily production not grazed by protists, we can partition the remaining carbon into major phytoplankton taxa to infer the fate of excess production (Fig. 14).

Clearly, the greatest excess of phytoplankton production was at southern stations during the SW Monsoon and northern coastal stations during the NE Monsoon, reflecting higher nutrient levels and the predominance of diatom species. As expected, there was little excess carbon production at offshore stations where nutrients were scarce, picoplankton dominated, and growth and grazing were in close agreement. While diatom growth comprised the majority of excess production across the region, a surprisingly large portion of *Synechococcus* spp. appeared to escape predation by protists. This may reflect some inefficiency in the degradation of their phycobiliprotein pigments, which would allow previously ingested cells to remain identifiable by FCM. Alternatively, we may have underestimated grazing losses to protists. Despite rapid daily population increases ($\mu > 2\,d^{-1}$) due to strong diel growth, Sherry and Wood (2001) document little change in cell abundances over 24-h cycles. In an earlier study, Burkill et al. (1993a,b) reported similar closely balanced growth and grazing mortality of *Synechococcus* spp. These inferred balances between

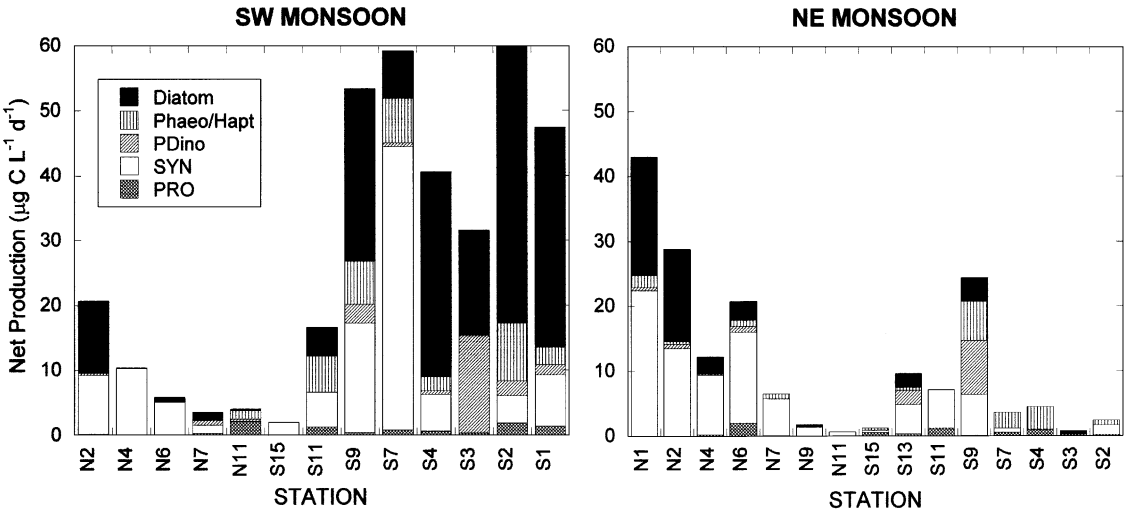

Fig. 14. Spatial distribution of net phytoplankton carbon production (*P–G*) and component taxa.

growth and grazing are at odds with our excess SYN production, suggesting grazing losses or mortality we have not accounted for. Diel variations in mixed layer depths and nocturnal mixing of excess surface production with deeper grazer populations could account for in situ grazing losses that were not measured in our incubations.

Excess diatom production during the SW Monsoon, particularly along the southern line ($\sim$50% of primary production) is consistent with the carbon demands of mesozooplankton. Roman et al. (2000) showed that mesozooplankton consumed 50% of integrated primary production during the SW Monsoon and $\sim$45% during the NE Monsoon. It should be noted, however, that these mesozooplankton ingestion rates included microzooplankton ($\sim$20% of carbon ingested) and detritus, such that the fraction of primary production actually consumed by mesozooplankton was $\leqslant$40% during the late SW Monsoon and $\leqslant$36% during the early NE Monsoon. Combined estimates of micro- and mesozooplankton grazing thus account for $\sim$90% of primary production at upwelling stations during the late SW Monsoon and 86–100% of production for northern and southern transect stations during the early NE Monsoon.

The combined effects of protist and mesozooplankton grazing leave $\sim$10% of primary production unaccounted for at upwelling stations during the SW Monsoon and 14% at northern stations during the NE Monsoon. At upwelling stations during the SW Monsoon and northern stations during the NE Monsoon, diatoms comprised a large fraction of production that escaped grazing by protists (Fig. 14), suggesting export by direct sinking as a possible mechanism for carbon removal. The appearance of senescent diatom cells during the late SW Monsoon (Garrison et al., 1998), as well as mucus-forming colonies of *Phaeocystis* spp., is consistent with aggregation and rapid sinking (Alldredge and Silver, 1988; Alldredge and Gotschalk, 1989; Passow and Wassmann, 1994; Wassmann, 1998). Roman et al. (2000) also found no relationship between POC flux and mesozooplankton fecal pellet production, suggesting an alternative mechanism for flux. The possibility of direct sinking of phytoplankton as a mechanism for flux is consistent with recent findings of fresh phytodetritus on the bottom of the abyssal Arabian Sea (Pfannkuche et al., 2000).

Export particle flux determined from sediment traps moored along the southern line showed a peak in both organic carbon and biogenic silica flux during the late SW Monsoon, consistent with the sinking of ungrazed diatoms and enhanced fecal pellet production (Honjo et al., 1999). Similarly, ^{234}Th-derived POC flux at 100 m

reached a maximum during this time (Buesseler et al., 1998a, b). We cannot compare our inferences of export flux at northern stations during the NE Monsoon as sediment traps were not located along the northern line and ^{234}Th-based fluxes were not measured there. However, we can reasonably speculate that export flux should have been enhanced relative to the rest of the region based on either the sinking of diatoms and/or grazing by mesozooplankton as the NE Monsoon developed.

It is difficult to compare rates of excess carbon production with POC flux estimates at 100 m in that our estimates represent only the surface mixed layer and did not always include the chlorophyll *a* maximum. In addition, ^{234}Th profiles of particle flux indicate that processes between the shallow mixed layer and 100 m are important in particle cycling (Buesseler et al., 1998a ,b). Nevertheless, our estimates of excess phytoplankton production at offshore oligotrophic stations are less than concurrent estimates of POC flux and appear to underestimate flux potential. Our estimates of production available for export do not account for the mesozooplankton–microzooplankton pathway, carnivory or detrital feeding, all of which serve to repackage and remove carbon in sinking fecal pellets, albeit inefficiently.

One plausible explanation for the discrepancy between our production estimates and POC flux at offshore stations are lateral advection of excess production from coastal waters via filaments and eddies (Brink et al., 1996; Manghnani et al., 1998; Flagg and Kim, 1998). Complex circulation patterns and mesoscale features characterize the Arabian Sea, and export flux may be dominated by these episodic events (Honjo et al., 1999). Advective transport of excess production from coastal waters to offshore sites would be consistent with estimates of grazing losses exceeding production at offshore stations. Alternatively, substantial accumulations of phytoplankton biomass at the chlorophyll *a* maximum below the mixed layer may contribute to measured POC flux at 100 m, but would not have been accounted for in our estimates of mixed-layer production. This alternative scenario was documented by Pollehne et al. (1993a, b) in which there was a strong vertical layering of larger, eukaryotic phytoplankton populations in the deep chlorophyll maximum underlying the picoplankton-dominated mixed-layer; this deep layer appeared to represent a large portion of the particle flux out of the photic zone.

In summary, we present here a composition of stocks and rates in an effort to evaluate factors influencing microbial dynamics, estimate total microbial production and partition production into component taxa. Our estimates of primary production were generally in good agreement with ^{14}C-uptake results, particularly during the SW Monsoon when biomass estimates were better constrained. Production by component taxa appeared to be controlled by different mechanisms; growth rates of *Synechococcus* spp. and diatoms appeared to be strongly limited by nutrient concentrations, while *Prochlorococcus* spp., dinoflagellates and *Phaeocystis* spp. were less so or not at all. The striking abundance of a tiny photosynthetic eukaryote at two coastal stations during the SW Monsoon demonstrates the importance of picoplankton in upwelling regions; however, the reasons for its limited distribution are not obvious. Microzooplankton consumed a greater proportion of production offshore and during the NE Monsoon, demonstrating their ability to more effectively graze and regulate the small prokaryotic phytoplankton in these regions. Net production of diatoms along the southern transect during the SW Monsoon was consistent with enhanced export flux and high abundances of mesozooplankton. Significant net production at northern coastal stations during both seasons suggests that this region may be an area of enhanced export flux as well. Marked spatial variability in microbial biomass and community structure and increases in net production reflect the influence of convective mixing, coastal upwelling and mesoscale features, leading to the episodic flux events that dominate export in this region.

Acknowledgements

This study was supported by NSF grants OCE 93-11246 (MRL and LC) and -10634 (DG and MMG). We thank the captain and crew of the R/V

Thomas G. Thompson for their assistance and professionalism in enjoyable and successful voyages. We acknowledge the cooperation and assistance of our many shipmates and colleagues, particularly the hydrography and nutrient teams led by J. Morrison and L. Codispoti. Special thanks goes to J. Constantinou, H. Nolla and H-B. Liu for cruise participation and sampling analyses. Finally, we are grateful to Sharon Smith for her organization, leadership and dedication without which the ASPS would have never happened. This manuscript was greatly improved by comments from three anonymous reviewers. This paper is US JGOFS contribution number 703 and number 5960 from the School of Ocean Earth Science and Technology, University of Hawaii at Manoa, Honolulu, HI.

References

Alldredge, A.L., Silver, M.W., 1988. Characteristics, dynamics and significance of marine snow. Progress in Oceanography 20, 41–82.

Alldredge, A.L., Gotschalk, C., 1989. Direct observations of the mass flocculation of diatom blooms: characteristics, settling velocities and formation of diatom aggregates. Deep-Sea Research I 36, 159–171.

Barber, R.T., Marra, J., Bidigare, R.R., Codispoti, L.A., Halpern, D., Johnson, Z., Latasa, M., Goericke, R., Smith, S.L., 2001. Primary productivity and its regulation in the Arabian Sea during 1995. Deep-Sea Research II 48, 1127–1172.

Bidigare, R.R., 1991. Analysis of algal chlorophylls and carotenoids. In: Hurd, D.C., Spencer, D.W. (Eds.), Marine Particles: Analysis and Characterization. American Geophysical Union, Washington DC, pp. 119–123 (Chapter 4).

Bidigare, R.R., Trees, C.C., 2000. HPLC phytoplankton pigments: sampling, laboratory methods, and quality assurance procedures. In: Fargion, G.S., Mueller, J.L. (Eds.), Ocean Optics Protocols for Satellite Ocean Color Sensor Validation, Revision 2, National Areonautical and Space Administration, Goddard Space Center, pp. 154–161.

Binder, B.J., Chisholm, S.W., Olson, R.J., Frankel, S.L., Worden, A.Z., 1996. Dynamics of picophytoplankton, ultraphytoplankton and bacteria in the central equatorial pacific. Deep-Sea Research II 43, 907–932.

Brink, K.H., Jones, B.H., Lee, C.M., Wood, M., 1996. A cool filament off Oman, June 1995: origins and fates of its water. EOS Transactions, AGU 77, F382.

Brown, S.L., Landry, M.R., Barber, R.T., Campbell, L., Garrison, D.L., Gowing, M.M., 1999. Picophytoplankton dynamics and production in the Arabian Sea during the 1995 Southwest Monsoon. Deep-Sea Research II 46, 1745–1768.

Brown, S.L., Landry, M.R., Neveux, J., Dupouy, C., in review. Microbial community abundance and biomass along a 180° transect in the equatorial Pacific during an ENSO cold phase. Journal of Geophysical Research, in review.

Buesseler, K., Ball, L., Andrews, J., Benitez-Nelson, C., Belastock, R., Chai, F., Chao, Y., 1998a. Upper ocean export of particulate organic carbon in the Arabian Sea derived from thorium-234. Deep-Sea Research II 45, 2461–2487.

Buesseler, K.O., 1998b. The de-coupling of production and particulate export in the surface ocean. Global Biogeochemical Cycles 12, 297–310.

Burkill, P.H., Mantoura, R.F.C., Owens, N.J.P., 1993a. Biogeochemical cycling in the northwestern Indian Ocean: a brief overview. Deep-Sea Research II 40, 643–649.

Burkill, P.H., Leakey, R.J.G., Owens, N.J.P., Mantoura, R.F.C., 1993b. *Synechococcus* and its importance to the microbial foodweb of the northwestern Indian Ocean. Deep-Sea Research II 40, 773–781.

Campbell, L., Landry, M.R., Constantinou, J.C., Nolla, H.A., Brown, S.L., Liu, H., Caron, D., 1998. Response of microbial community structure to environmental forcing in the Arabian Sea. Deep-Sea Research II 45, 2301–2325.

Carlson, C.A., Ducklow, H.W., 1995. Dissolved organic carbon in the upper ocean of the central equatorial Pacific Ocean, 1992: daily and finescale vertical variations. Deep-Sea Research II 42, 639–654.

Chavez, F.P., Buck, K.R., Service, S.K., Newton, J., Barber, R.T., 1996. Phytoplankton variability in the central and eastern tropical pacific. Deep-Sea Research II 43, 835–870.

Chretiennot-Dinet, M.-J., Courties, C., Vaquer, A., Neveux, J., Claustre, H., Lauther, J., Machado, M.C., 1995. A new marine picoeucaryote: *Ostreococcus tauri.* gen. et sp. nov. (Chlorophyta, Prasinophyceae). Phycologia 34, 285–292.

Constantinou, J., 1994. Mixotrophic nanoflagellates in marine microbial food webs. M.S. Thesis, Department of Oceanography, University of Hawaii, Manoa, 36pp.

Courties, C., Vaquer, A., Troussellier, M., Lautier, J., Chretiennot-Dinnet, M.J., Neveux, J., Machado, C., Claustre, H., 1994. Smallest eukaryotic organism. Nature 370, 255.

Courties, C., Perasso, R., Chretiennot-Dinet, M.J., Guoy, M., Guillou, L., Troussellier, M., 1998. Phylogenetic analysis and genome size of *Ostreococcus tauri* (Chlorophyta, Prasinophyceae). Journal of Phycology 34, 844–849.

Dam, H.G., Roman, M.R., Youngbluth, M.J., 1995. Downward export of respiratory carbon and dissolved inorganic nitrogen by diel-migrant mesozooplankton at the JGOFS Bermuda time-series station. Deep-Sea Research II 42, 1187–1197.

Dickey, T., Marra, J., Sigurdson, D.E., Weller, R.A., Kinkade, C.S., Zedler, S.E., Wiggert, J.D., Langdon, C., 1998. Seasonal variability of bio-optical and physical properties in the Arabian Sea: October 1994–October 1995. Deep-Sea Research II 45, 2001–2025.

Dickson, M-L., Orchardo, J., Barber, R.T., Marra, J., McCarthy, J.J., Sambrotto, R., 2001. Production and respiration rates in the Arabian Sea during the 1995 Northeast and Southwest Monsoons. Deep-Sea Research II 48, 1199–1230.

Ducklow, H.W., Smith, D.C., Campbell, L., Landry, M.R., Quinby, H.L., Steward, G., Azam, F., 2001. Heterotrophic bacterioplankton distributions in the Arabian Sea: basin-wide response to year-round high primary productivity. Deep-Sea Research II 48, 1303–1324.

Eppley, R.W., Reid, F.M.H., Strickland, J.D.H., 1970. Estimates of phytoplankton crop size, growth rate, and primary production. In: Strickland, J.D.H. (Ed.), The Ecology of the Plankton Off La Jolla California in the Period April Through September, Vol. 17, 1967. Bulletin of Scripps Institution of Oceanography, pp. 33–42.

Fenchel, T., 1982. Ecology of heterotrophic microflagellates. I. Some important forms and their functional morphology. Marine Ecology Progress Series 8, 211–223.

Fenchel, T., 1984. Suspended marine bacteria as a food source. In: Fasham, M.J. (Ed.), Flow of Material and Energy in Marine Ecosystems. Plenum Press, New York, pp. 301–315.

Ferguson, R.L., Buckley, E.N., Palumbo, A.V., 1984. Response of marine bacterioplankton to differential filtration and confinement. Applied and Environmental Microbiology 47, 49–55.

Flagg, C.N., Kim, H.-S., 1998. Upper ocean currents in the northern Arabian Sea from shipboard ADCP measurements collected during the 1994–1996 US JGOFS and ONR programs. Deep-Sea Research II 45, 1917–1960.

Gardner, W.D., Gundersen, J.S., Richardson, M.J., Walsh, I.D., 1999. The role of seasonal and diel changes in mixed-layer on carbon and chlorophyll distributions in the Arabian Sea. Deep-Sea Research II 46, 1833–1858.

Garrison, D.L., Gowing, M.M., Hughes, M.P., 1998. Nano- and microplankton in the northern Arabian Sea during the Southwest Monsoon, August–September, 1995: A US-JGOFS study. Deep-Sea Research II 45, 2269–2300.

Garrison, D.L., Gowing, M.M., Hughes, M.P., Campbell, L., Caron, D.A., Dennett, M.R., Shalapyonok, A., Olson, R.J., Landry, M.R., Brown, S.L., Liu, H., Azam, F., Steward, G.F., Ducklow, H.W., Smith, D.C., 2000. Microbial food web structure in the Arabian Sea: a US JGOFS study. Deep-Sea Research II 47, 1387–1422.

Gifford, D.J., Dagg, M.J., 1991. The microzooplankton–mesozooplankton link: consumption of planktonic protozoa by the calanoid copepods *Acartia tonsa* Dana and *Neocalanus plumchrus* Murukawa. Marine Microbial Food Webs 5, 161–177.

Goericke, R., Welschmeyer, N.A., 1992a. Pigment turnover in the marine diatom *Thalassiosira weissflogii*. I. The $^{14}CO_2$-labeling kinetics of chlorophyll *a*. Journal of Phycology 28, 498–507.

Goericke, R., Welschmeyer, N.A., 1992b. Pigment turnover in the marine diatom *Thalassiosira weissflogii*. II. The $^{14}CO_2$-labeling kinetics of carotenoids. Journal of Phycology 28, 507–517.

Gonzales, J.M., Sherr, E.B., Sherr, B.F., 1990. Size-selective grazing on bacteria by natural assemblages of estuarine flagellates and ciliates. Applied Environmental Microbiology 56, 583–589.

Honjo, S., Dymond, J., Prell, W., Ittekkot, V., 1999. Monsoon-controlled export fluxes to the interior of the Arabian Sea. Deep-Sea Research II 46, 1859–1901.

Jochem, F.J., Pollehne, F., Zeitzschel, B., 1993. Productivity regime and phytoplankton size structure in the Arabian Sea. Deep-Sea Research II 40, 711–735.

Karl, D.M., 1986. Determination of in situ microbial biomass, viability, metabolism and growth. In: Poindexter, J.S., Leadbetter, E.R. (Eds.), Bacteria in Nature, Vol. 2. Plenum Publishing Corporation, New York, pp. 85–176.

Kim, H.-S., Flagg, C.N., Howden, S.D., 2001. Northern Arabian Sea variability from TOPEX/Poseidon altimetry data: an extension of the US JGOFS/ONR shipboard ADCP study. Deep-Sea Research II 48, 1069–1096.

Klein, B., Gieskes, W.C., Kraay, G.C., 1986. Digestion of chlorophylls and carotenoids by the marine protozoa *Oxyrrhis marina* studied by h.p.l.c. analysis of algal pigments. Journal of Plankton Research 8, 827–836.

Kleppel, G.S., 1992. Environmental regulation of feeding and egg production by *Acartia tonsa* off southern California. Marine Biology 112, 57–65.

Landry, M.R., 1993. Estimating rates of growth and grazing of phytoplankton by dilution. In: Kemp, P.K., Sherr, B.F., Sherr, E.B., Jonathan, J.C. (Eds.), Handbook of Methods in Aquatic Microbial Ecology. CRC Press, Boca Raton, Fl, pp. 715–722.

Landry, M.R., Hassett, R.P., 1982. Estimating the grazing impact of marine microzooplankton. Marine Biology 67, 283–288.

Landry, M.R., Kirchman, D.L., 2002. Microbial community structure and variability in the tropical Pacific. Deep-Sea Research II, in press.

Landry, M.R., Kirshtein, J., Constantinou, J., 1995. A refined dilution technique for measuring the community grazing impact of microzooplankton, with experimental tests in the central equatorial Pacific. Marine Ecology Progress Series 120, 53–63.

Landry, M.R., Brown, S.L., Campbell, L., Constantinou, J., Liu, H., 1998. Spatial patterns in phytoplankton growth and microzooplankton grazing in the Arabian Sea during monsoonal forcing. Deep-Sea Research II 45, 2353–2368.

Landry, M.R., Constantinou, J., Latasa, M., Brown, S.L., Bidigare, R.R., Ondrusek, M., 2000. Biological response to iron fertilization in the eastern equatorial Pacific (IronEx II). III. Dynamics of phytoplankton growth and microzooplankton grazing. Marine Ecology Progress Series 201, 57–72.

Landry, M.R., Selph, K.E., Brown, S.L., Abbott, M.R., Measures, C.I., Vink, S., Allen, C.B., Calbet, A., Christensen, S., Nolla, H., 2002. Seasonal dynamics of phytoplankton in the Antarctic Polar Front region at 170°W. Deep-Sea Research II 49, 1843–1865.

Landry, M.R., Brown, S.L., Neveux, J., Dupouy, C., Blanchot, J., Christensen, S., Bidigare, R.R., submitted. Phytoplankton growth and microzooplankton grazing in HNLC waters of the equatorial Pacific: community and taxon-specific rate assessments from pigment and flow cytometric analyses. Journal of Geophysical Research, submitted.

Latasa, M., Bidigare, R.R., 1998. A comparison of phytoplankton populations of the Arabian Sea during the Spring Intermonsoon and Southwest Monsoon of 1995 as described by HPLC-analyzed pigments. Deep-Sea Research II 45, 2133–2170.

Laws, E.A., 1984. Improved estimates of phytoplankton carbon based on ^{14}C incorporation into chlorophyll *a*. Journal of Theoretical Biology 110, 425–434.

Laws, E.A., Landry, M.R., Barber, R.T., Campbell, L., Dickson, M-L., Marra, J., 2000. Carbon cycling in primary production bottle incubations: inferences from grazing experiments and photosynthetic studies using ^{14}C and ^{18}O in the Arabian Sea. Deep-Sea Research II 47, 1339–1352.

Lee, C.M., Jones, B.H., Brink, K.H., Fischer, A.S., 2000. The upper-ocean response to monsoonal forcing in the Arabian Sea: seasonal and spatial variability. Deep-Sea Research II 47, 1177–1226.

Liu, H., Campbell, L., Landry, M.R., Nolla, H.A., Brown, S.L., Constantinou, J., 1998. *Prochlorococcus* and *Synechococcus* growth rates and contributions to production in the Arabian Sea during the 1995 Southwest and Northeast Monsoons. Deep-Sea Research II 45, 2327–2352.

Manghnani, V., Morrison, J.M., Hopkins, T.S., Bohm, E., 1998. Advection of upwelled waters in the form of plumes off Oman during the Southwest Monsoon. Deep-Sea Research II 45, 2027–2052.

Monger, B.C., Landry, M.R., 1990. Direct-interception feeding by marine zooflagellates: the importance of surface and hydrodynamic forces. Marine Ecology Progress Series 65, 123–140.

Monger, B.C., Landry, M.R., 1991. Prey-size dependency of grazing by free-living marine flagellates. Marine Ecology Progress Series 74, 239–248.

Monger, B.C., Landry, M.R., 1993. Flow cytometric analysis of marine bacteria with Hoechst 33342. Applied Environmental Microbiology 59, 905–911.

Morel, A., 1991. Optics of marine particles and marine optics. In: Demers, S. (Ed.), Particle Analysis in Oceanography. NATO ASI Series G, Ecological Sciences, Vol. 27. Springer, New York, pp. 141–188.

Morrison, J., Codispoti, L.A., Gaurin, S., Jones, B., Manghnani, V., Zheng, Z., 1998. Seasonal variation of hydrographic and nutrient fields during the US JGOFS Arabian Sea Process study. Deep-Sea Research II 45, 2053–2102.

Passow, U., Wassmann, P., 1994. On the trophic fate of *PHAEOCYSTIS pouchetti* (hariot): IV. The formation of marine snow by *Pouchetti*, *P*. Marine Ecology Progress Series 104, 153–161.

Pfannkuche, O., Sommer, S., Kähler, A., 2000. Coupling between phytodetritus deposition and the small-sized benthic biota in the deep Arabian Sea: analysis of biogenic sediment compounds. Deep-Sea Research II 47, 2805–2833.

Pollehne, F., Klein, B., Zeitschel, B., 1993a. Low light adaptation and export production in the deep chlorophyll maximum layer in the northern Indian Ocean. Deep-Sea Research II 40, 737–752.

Pollehne, F., Zeitschel, B., Peiner, R., 1993b. Short-term sedimentation patterns in the northern Indian Ocean. Deep-Sea Research II 40, 833–849.

Putt, M., Stoecker, D.K., 1989. An experimentally determined carbon: volume ratio for marine 'oligotrichous' ciliates from estuarine and coastal waters. Limnology and Oceanography 34, 1097–1103.

Roman, M., Gauzens, A.L., 1997. Copepod grazing in the equatorial Pacific. Limnology and Oceanography 42, 623–634.

Roman, M., Smith, S.L., Wishner, K., Zhang, X., Gowing, M., 2000. Mesozooplankton production and grazing in the Arabian Sea. Deep-Sea Research II 47, 1423–1450.

Rousseau, V., Mathot, S., Lancelot, C., 1990. Calculating carbon biomass of *Phaeocystis* spp. from microscopic observations. Marine Biology 107, 305–314.

Shalapyonok, A., Olson, R.J., Shalapyonok, L.S., 2001. Arabian Sea phytoplankton during the Southwest and Northeast Monsoons 1995: composition, size structure, and biomass from individual cell properties measured by flow cytometry. Deep-Sea Research II 48, 1231–1261.

Sherry, N.D., Wood, A.M., 2001. Phycoerythrin-containing picocyanobacteria in the Arabian Sea in February 1995: diel patterns, spatial variability, and growth rates. Deep-Sea Research II 48, 1263–1284.

Shiah, F.-K., Ducklow, H.W., 1997. Bacterioplankton growth responses to temperature and chlorophyll variations in estuaries measured by thymidine:leucine incorporation ratio. Aquatic Microbial Ecology 13, 151–159.

Smith, S., Codispoti, L., Morrison, J., Barber, R.T., 1998a. The 1994–1996 Arabian Sea Expedition: an integrated, interdisciplinary investigation of the response of the northwestern Indian Ocean to monsoonal forcing. Deep-Sea Research II 45, 1905–1916.

Smith, S.L., Roman, M., Prusova, I., Wishner, K., Gowing, M., Codispoti, L.A., Barber, R., Marra, J., Flagg, C., 1998b. Seasonal response of zooplankton to monsoonal reversals in the Arabian Sea. Deep-Sea Research II 45, 2369–2403.

Stelfox, C.E., Burkill, P.H., Edwards, E.S., Harris, R.P., Sleigh, M.A., 1999. The structure of zooplankton communities, in the 2 to 2000 μm size range, in the Arabian Sea during and after the SW monsoon, 1994. Deep-Sea Research II 46, 815–841.

Stoecker, D.K., Capuzzo, J.M., 1990. Predation on protozoa: its importance to zooplankton. Journal of Plankton Research 12, 891–908.

Strom, S.L., 1993. Production of phaeopigments by marine protozoa: results of laboratory experiments analyzed by HPLC. Deep-Sea Research I 40, 57–80.

Tarran, G.A., Burkill, P.H., Edwards, E.S., Woodward, E.M.S., 1999. Phytoplankton community structure in the Arabian Sea during and after the SW monsoon. Deep-Sea Research II 46, 655–675.

Thomas, W.H., Gibson, C.H., 1990. Quantified small-scale turbulence inhibits a red tide dinoflagellate, *Gonyaulax polyedra* Stein. Deep-Sea Research I 37, 1583–1593.

Tremaine, S.C., Mills, A.L., 1987. Tests of the critical assumptions of the dilution method for estimating bacterivory by microeucaryotes. Applied and Environmental Microbiology 53, 2914–2921.

Vaulot, D., Marie, D., Olson, R.J., Chisholm, S.W., 1995. Growth of *Prochlorococcus*, a photosynthetic prokaryote, in the equatorial Pacific Ocean. Science 268, 1480–1482.

Verity, P., Paffenhoffer, G.-A., 1996. On assessment of prey ingestion by copepods. Journal of Plankton Research 18, 1767–1779.

Wassmann, P., 1998. Retention versus export food chains: processes controlling sinking losses from marine pelagic systems. Hydrobiologia 363, 29–57.

Waterhouse, T.Y., Welschmeyer, N.A., 1995. Taxon-specific analysis of microzooplankton grazing rates and phytoplankton growth rates. Limnology and Oceanography 40, 827–834.

Wright, S.W., Jeffrey, S.W., Mantoura, R.F.C., Llewellyn, C.A., Bjornland, T., Repeta, D., Welschmeyer, N., 1991. Improved HPLC method for the analysis of chlorophylls and carotenoids from marine phytoplankton. Marine Ecology Progress Series 77, 183–196.